EFFECTS OF TEMPERATURE DEPENDENT THERMAL CONDUCTIVITY ON MAGNETOHYDRODYNAMIC FREE CONVECTION FLOW ALONG A VERTICAL FLAT PLATE WITH HEAT GENERATION

by

MOZZEM HOSSAIN
Student No. 100609002P
Registration No.100609002, Session: October-2006

MASTER OF PHILOSOPHY
IN
MATHEMATICS

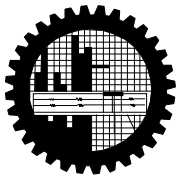

Department of Mathematics
Bangladesh University of Engineering & Technology
Dhaka-1000, Bangladesh
September, 2011

The thesis titled

EFFECTS OF TEMPERATURE DEPENDENT THERMAL CONDUCTIVITY ON MAGNETOHYDRODYNAMIC FREE CONVECTION FLOW ALONG A VERTICAL FLAT PLATE WITH HEAT GENERATION

Submitted by

MOZZEM HOSSAIN

Student No.100609002P, Registration No.100609002, Session: October-2006, a part-time student of M. Phil. (Mathematics) has been accepted as satisfactory in partial fulfillment for the degree of

Master of Philosophy in Mathematics

on September 17, 2011

BOARD OF EXAMINERS

1. _____
Dr. Md. Abdul Alim — Chairman
Associate Professor — (Supervisor)
Department of Mathematics, BUET, Dhaka

2. _____
Head — Member
Department of Mathematics, BUET, Dhaka — (Ex-Officio)

3. _____
Dr. Md. Mustafa Kamal Chowdhury — Member
Professor
Department of Mathematics, BUET, Dhaka

4. _____
Md. Obayedullah — Member
Associate Professor
Department of Mathematics, BUET, Dhaka

5. _____
Dr. K.C. Amanul Alam — Member
Associate Professor — (External)
Department of Electronics and Communications Engineering
East West University, Dhaka

DEDICATION

This work is dedicated

To

My beloved parents

Abstract

The conjugate effects of temperature dependent thermal conductivity on Magnetohydrodynamic free convection flow along a vertical flat plate with heat generation and pressure work have been investigated. The governing equations with associated boundary conditions for this phenomenon are converted to dimensionless form using suitable transformations, the governing equations containing the equation of continuity, momentum and energy. The transformed non-linear system of partial differential equations is then solved using the implicit finite difference method with H. B. Keller (1978)–box scheme. FORTRAN 90 is used to perform computational job and the post processing software TECHPLOT has been used to display the numerical results graphically. Numerical results of the velocity profiles, temperature profiles, skin friction co-efficient and surface temperature distribution for different values of the magnetic parameter M, Prandtl number Pr, thermal conductivity variation parameter γ, heat generation parameter Q and pressure work parameter ε are presented graphically. Detailed discussion is given for the effects of the aforementioned parameters.

Author's Declaration

I hereby declare that this thesis work submitted to the Department of Mathematics, Bangladesh University of Engineering and Technology (BUET) in partial fulfillment of the requirements for the degree of Master of Philosophy in Mathematics has not been submitted elsewhere (Universities or Institutions) for the any other degree.

Mozzem Hossain

Date: September 17, 2011

Acknowledgements

All praises are due to the almighty Allah Who deserves credits for successful completion of this thesis.

I feel it a proud privilege to extend my profound respect, deepest sense of intense gratitude, indebtedness and regards to my reverend supervisor Dr. Md. Abdul Alim, Associate Professor, Department of Mathematics, BUET, Dhaka for his invaluable guidance, constructive advice and suggestions to carry out the research work towards successful completion and in preparation of this thesis.

I am pleased to avail myself to express my heartfelt gratitude, ever indebtedness and deep felicitation to Prof. Dr. Abdul Hakim Khan, Head, Department of Mathematics, Prof. Dr. Mustafa Kamal Chowdhury and Prof. Dr. Abdul Maleque, the former Head of the Department of Mathematics, Prof. Dr. Monirul Alam Sarker and Md. Obayedullah Department of Mathematics, BUET, Dhaka for their wise and liberal co-operation in providing me all necessary help from the department during my course of M. Phil. Program. I desire to express my profound appreciation and respect to all my respectable teachers, Department of Mathematics, BUET, Dhaka for their constant encouragement, scholastic guidance, untiring assistance and inspiration to accomplish the study and to help in preparing the manuscript of this thesis. I wish to acknowledge to my classmates who had tremendously and positively inspired me.

Diction is not enough to express my profound gratitude and deepest appreciation to my parents for their never ending prayer, and sacrifice to educate me to this level.

Contents

Nomenclature

b	Plate thickness
C_{fx}	Local skin friction coefficient
C_{p}	Specific heat at constant pressure
f	Dimensionless stream function
g	Acceleration due to gravity
Gr	Grashof number
h	Dimensionless temperature
H_0	Applied magnetic field strength
$\bar{J}$	Current density vector
l	Length of the plate
L	Reference length
M	Magnetic parameter
p	Conjugate conduction parameter
Pr	Prandtl number
Q	Heat generation parameter
T	Temperature of the interface
T_b	Temperature at outside surface of the plate
T_f	Temperature of the fluid
T_∞	Temperature of the ambient fluid
$\bar{u}$	Velocity component in x- direction
$\bar{v}$	Velocity component in y- direction
u	Dimensionless velocity component in x- direction
v	Dimensionless velocity component in y- direction
$\bar{x}$	Cartesian co-ordinates
$\bar{y}$	Cartesian co-ordinates
x	Dimensionless Cartesian co-ordinates
y	Dimensionless Cartesian co-ordinates

Greek Symbols

β	Co-efficient of thermal expansion
γ	Thermal conductivity variation parameter
ε	Pressure work parameter
δ	Constant
η	Similarity variable
$\theta(x,0)$	Surface temperature profile
κ_∞	Thermal conductivity of the ambient fluid
κ_s	Thermal conductivity of the solid
κ_f	Thermal conductivity of the fluid
μ	Viscosity of the fluid
ν	Kinematic viscosity
ρ	Density of the fluid inside the boundary layer
ρ_∞	Density of the fluid outside the boundary layer
τ_w	Shearing stress
ψ	Stream function

List of Tables

List of Figures

Chapter 1

Introduction

1.1 General

Fluid dynamics is one of the oldest branches of applied mathematics which is concerned with the study of the motion of fluids or that of bodies in contact with fluids. It is also the branch in which some of the most significant advances have been made during the last fifty years. These advances have been motivated by exciting development in science and technology and facilitated by growth of computer capabilities and developments of sophisticated mathematical techniques.

Heat is the form of energy that can be transferred from one system to another as a result of temperature difference. A thermodynamic analysis is concerned with the amount of heat transfer as a system undergoes a process from one equilibrium state to another. The science that deals with the determination of the rates of such energy transfers is the heat transfer. The transfer of energy as heat is always from the higher temperature medium to the lower temperature one, and heat transfer stops when the two mediums reach the same temperature. Heat transfer is that science which seeks to predict the energy transfer which may take place between material bodies as a result of a temperature difference. Thermodynamics teaches that this energy transfer is defined as heat. The science of heat transfer seeks not merely to explain how heat energy may be transferred, but also to predict the rate at which the exchange will take place under certain specified conditions.

The phenomenon of heat transfer was known to human being even in the primitive age when they used to use solar energy as a source of heat. Heat transfer in its initial stage was conceived with the invention of fire in the early age of human civilization. Since then its knowledge and use has been progressively increasing each day as it is directly related to the growth of human civilization. With the invention of stream engine by James watt in 1765 A. D., the phenomenon of heat transfer got its first industrial recognition and after that its use extended to a great extent and spread out in different spheres of engineering fields. In the past three decades, digital computers, numerical techniques and development of numerical models of heat transfer have made it possible to calculate heat transfer of considerable complexity and thereby create a new approach

to the design of heat transfer equipment. Heat transfer processes have always been an integral part of our environment.

The study of temperature and heat transfer is of great importance to the engineers because of its almost universal occurrence in many branches of science and engineering. Although heat transfer analysis is most important for the proper sizing of fuel elements in the nuclear reactors cores to prevent burnout, the performance of aircraft also depends upon the case with which the structure and engines can be cooled. The design of chemical plants is usually done on the basis of heat transfer analysis and the analogous mass transfer processes. The transfer and conversion of energy from one form to another is the basis to all heat transfer process and hence, they are governed by the first as well as the second law of thermodynamics. Heat transfer is commonly associated with fluid dynamics. The knowledge of temperature distribution is essential in heat transfer studies because of the fact that the heat flow takes place only wherever there is a temperature gradient in a system. The heat flux which is defined as the amount of heat transfer per unit area in per unit time can be calculated from the physical laws relating to the temperature gradient and the heat flux.

Heat can be transferred in three different mechanisms or modes: conduction, convection and radiation. All modes of heat transfer require the existence of a temperature difference, and all modes are from the high temperature medium to a lower temperature one. In reality, the combined effect of these three modes of heat transfer control temperature distribution in a medium. Conduction is most effective in solids but it can happen in fluids. Also Radiation Electromagnetic waves that directly transports energy through space. Sunlight is a form of radiation that is radiated through space to our planet without the aid of fluids or solids. The sun transfers heat through 93 million miles of space. Because there are no solids touching the sun and our planet, conduction is not responsible for transferring the heat. Thus radiation brings heat to our planet.

1.2 Some Definitions

Some basic definitions that are related to this study are presented below.

Convection

Convective heat transfer or, simply, convection is the study of heat transport processes affected by the flow of fluids. Convection is that mode of heat transfer where energy exchange occurs between the particles by convection current. It may be explained as; when fluid flows over a solid body or inside a channel while temperatures of the fluid and the solid surface are different, heat transfer between the fluid and the solid surface takes place as a consequences of the motion of the fluid relative to the surfaces; the mechanism of heat transfer called convection. The convection mode of heat transfer is further divided into two basic processes. If the motion of the fluid arises due to an external agent, such as the externally imposed flow of fluid stream over a heated object, the process is termed as forced convection. The fluid flow may be the results of, for instance, a fan, a blower, the wind or the motion of the heated object itself. Such problems are very frequently encountered in technology where heat transfer to, or from, a body is often due to an imposed flow of a fluid at a temperature different from that of the body. It has wide applications in compact heat exchanger, central air conditioning system, cooling tower, gas turbine blade, internal cooling passage, chemical engineering process industries, nuclear reactors and many other cases. If, on the other hand, no such externally induced flow is provided and the flow arises “naturally” simply due to the effect of a density difference, resulting from a temperature difference, in a body force field, such as gravitational field, the process is termed as natural or free convection. The density deference gives rise to buoyancy effects due to which the flow is generated. A heated body cooling in ambient air generates such a flow in the region surrounding it. Similarly, the buoyant flow arising from heat rejection to the atmosphere and to other ambient media, Heat transfer by free convection occurs in many engineering applications, such as heat transfer from hot radiators, refrigerator coils, transmission lines, electric transformers, electric heating elements and electronic equipment etc.

The convection heat transfer that is neither dominated by pure forced nor pure free convection, but is rather a combination of the two is referred as combined or mixed convection. The buoyancy forces that arise as the results of the temperature differences and which cause the fluid flow in free convection also exist when there is a forced flow.

The effects of these buoyancy forces are however; usually negligible when there is a forced flow. In some cases, however, these buoyancy forces do have a significant influence on the flow and consequently on the heat transfer rate. In such cases, the flow about the body is a combination of forced and free convection; such flows are referred to as mixed convection. For example, heat transfer from one fluid to another fluid through the walls of pipe occurs in many practical devices. In this case, heat is transferred by convection from the hotter fluid to the one surface of the pipe. Heat is then transferred by conduction through the walls of the pipe. Finally, heat is transferred by convection from the other surface to the colder fluid.

Magnetohydronamics

Magnetohydrodynamics (MHD) is that branch of science, which deals with the motion of highly conducting ionized (electric conductor) fluid like mercury in presence of magnetic field. The motion of the conducting fluid across the magnetic field generates electric currents which change the magnetic field and the action of the magnetic field on these currents give rise to mechanical forces, which modify the fluid. It is possible to attain equilibrium in a conducting fluid if the current is parallel to the magnetic field for then the magnetic forces vanish and the equilibrium of the gas is the same as in the absence of magnetic fields. But most liquids and gases are poor conductors of electricity. In the case when the conductor is either a liquid or a gas, electromagnetic forces will be generated which may be of the same order of magnitude as the hydrodynamical and inertial forces. Thus the equation of motion as well as the other forces will have to take these electromagnetic forces into account. The MHD was originally applied to astrophysical and geophysical problems, where it is still very important but more recently applied to the problem of fusion power where the application is the creation and containment of hot plasmas by electromagnetic forces, since material walls would be destroyed. Astrophysical problems include solar structure, especially in the outer layers, the solar wind bathing the earth and other planets and interstellar magnetic fields. The primary geophysical problem is planetary magnetism, produced by currents deep in the planet, a problem that has not been solved to any degree of satisfaction.

Thermal Conductivity

Thermal conductivity of a material can be defined as the rate of heat transfer through a unit thickness of the material per unit area per unit temperature difference. Therefore the thermal conductivity of a material is a measure of the ability of the material to conduct heat. A high value for thermal conductivity indicates that the material is a good heat conductor, and a low value for thermal conductivity indicates that the material is a poor heat conductor or insulator. For example the materials such as copper and silver that are good electric conductors are also good heat conductors, and have high values of thermal conductivity. Materials such as rubber, wood are poor conductors of heat and have low conductivity values. The rate of heat conduction through a medium depends on the geometry of the medium, its thickness, and the material of the medium, as well as the temperature difference across the medium. According to Fourier's law (1955), the rate of heat conduction is proportional to the area-measured normal to the direction of heat flow and to the temperature gradient in that direction

$$Q = -\kappa A \frac{\partial T}{\partial n} \quad \text{or} \quad q = -\kappa \frac{\partial T}{\partial n} \tag{1}$$

The constant of proportionality κ is called the coefficient of thermal conductivity, which is a physical property of the substance and is defined as the ability of a substance to conduct heat. Since conduction is a molecular phenomenon, Fourier's law (1) is similar to Newton's viscosity law for laminar flow $\tau = \mu \frac{\partial u}{\partial y}$ (2)

Comparing equations (1) and (2) we note that the viscosity in fluid motion is analogous to the thermal conductivity in heat transfer. Thermal conductivity like viscosity is primarily a function of temperature and / or position and nature of the substance. It varies significantly with pressure only in the case of gases subjected to high pressure. However, for many engineering problems, materials are often considered to possess a constant thermal conductivity (isotropic). Pure metals have the height values of thermal conductivity while gasses and vapors have the lowest. For most pure metals thermal conductivity decreases with increasing temperature where as for gases and insulating material it increases with increasing temperature.

Heat Generation

A medium through which heat is conducted may involve the conversation of electrical, nuclear or chemical energy into heat (or thermal) energy. In heat conduction analysis, such conversion processes are characterized as heat generation. For example, the temperature of a resistance wire rises rapidly when electric current posses through it as a result of the electrical energy are converted to heat at a rate of I^2R, where I is the current and R is the electrical resistance of the wire. The safe and effective removal of this heat away from the sites of heat generation (the electronic circuits) is the subject of electronics cooling which is one of the modern application areas of heat transfer. Likewise, a large amount of heat is generated in the fuel elements of nuclear reactors as a result of nuclear fission that serves as the heat source for the nuclear power plants. The heat generated in the sun as a result of the fusion of hydrogen into helium makes the sun a large nuclear reactor that supplies heat to the earth. Another source of heat generation in a medium is exothermic chemical reactions that may occur throughout the medium. The chemical reaction in this case serves as a heat source for the medium. In the case of endothermic reactions, however, heat is absorbed instead of being released during reaction and thus the chemical reaction serves as a heat sink. The heat generation term becomes a negative quantity in this case. Heat generation is a volumetric phenomenon. That is, it occurs throughout the body of a medium. Therefore, the rate of heat generation in a medium is usually specified per unit volume.

Pressure work

The rate at which the pressure does work known as a pressure work on one side of a moving flat surface in the fluid is the product of the pressure, the area of the surface and the normal component of velocity. Thus rate of doing work = Force (due to pressure) × velocity.

Thus pressure work = $Tu\beta\dfrac{\partial p}{\partial x}$, where T, β are the temperature and volumetric thermal expansion respectively.

The work done by the system against pressure, which is also called flow work. The rate of work done by the system against pressure acting at a surface element dA_{out} will be given by $pdA_{out}.\hat{n}$, Where p is the pressure acting on the surface element. Therefore, the

rate of work done against pressure over A_{out} is $\int A_{out} pV.\hat{n}dA_{out}$. Similarly, the rate of work done on the system by pressure acting on A_{in} would be given by $-\int A_{in} pV.\hat{n}dA_{in}$. Thus the network done by the system against pressure will be

$$\int A_{out} pV.\hat{n}dA_{out} - \int A_{in} pV.\hat{n}dA_{in} = \int_{c.s} pV.\hat{n}dA$$

Thermal Diffusivity

The time dependent heat conduction equation for constant k contains a quantity α, called the thermal diffusivity of the material. Thermal diffusivity represents how fast heat diffuses through a material and is defined as

$$\alpha = \frac{\kappa}{\rho C_p}$$

Here the thermal conductivity κ represents how well a material conducts heat, and the heat capacity ρCp represents how much energy a material stores per unit volume. Therefore, the thermal diffusivity of a material can be viewed as the ratio of the heat conducted through the material to the heat stored per unit volume. A material that has a high thermal conductivity or a low heat capacity will obviously have a large thermal diffusivity. The larger thermal diffusivity means that the propagation of heat into the medium is faster. A small value of thermal diffusivity means the material mostly absorbs the heat and a small amount of heat is conducted further. It has got the units (m^2/s) or (L^2/t). The physical significance of thermal diffusivity is that it tells us how fast heat is propagated or it diffuses through a material during change of temperature with time. The large the thermal diffusivity, the shorter is the time required for the applied heat to penetrate deeper into the solid.

Boundary Layer

Since fluid motion is the distinguishing feature of heat convection, it is necessary to understand some of the principles of fluid dynamics in order to describe adequately the processes of convection. When a fluid flows over a body, the velocity and temperature distribution at the immediate vicinity of the surface strongly influence by the convective heat transfer. In order to simplify the analysis of convective heat transfer the boundary layer concept frequently is introduced to model the velocity and temperature fields near

the solid surface in order to simplify the analysis of convective heat transfer. So we are concerned with two different kinds of boundary layers, the velocity boundary layer and the thermal boundary layer.

The velocity boundary layer is defined as the narrow region, near the solid surface, over which velocity gradients and shear stresses are large, but in the region outside the boundary layer, called the potential-flow region, the velocity gradients and shear stresses are negligible. The exact limit of the boundary layer cannot be precisely defined because of the asymptotic nature of the velocity variation. The limit of the boundary layer is usually taken to be at the distance from the surface, at which the fluid velocity is equal to a predetermined percentage of the free stream value, U_∞. This percentage depends on the accuracy desired, 99 or 95% being customary. Although, outside the boundary layer region the flow is assumed to be inviscid, but inside the boundary layer the viscous flow may be either laminar or turbulent. In the case of laminar boundary layer, fluid motion is highly ordered and it is possible to identify streamlines along which particles move. Fluid motion along a streamline is characterized by velocity components in both the x and y directions. Since the velocity component v is in the direction normal to the surface, it can contribute significantly to the transfer of momentum, energy or species through the boundary layer. Fluid motion normal to the surface is necessitated by boundary layer growth in the x direction. In contrast, fluid motion in the turbulent boundary layer is highly irregular and is characterized by velocity fluctuations. These fluctuations enhance the transfer of momentum, energy and species and hence increase surface friction, as well as convection transfer rates. Due to fluid mixing resulting from the fluctuations, turbulent boundary layer thicknesses are larger and boundary layer profiles are flatter than in laminar flow. The thermal boundary layer may be defined (in the same sense that the velocity boundary layer was defined above) as the narrow region between the surface and the point at which the fluid temperature has reached a certain percentage of ambient temperature T_∞. Outside the thermal boundary layer the fluid is assumed to be a heat sink at a uniform temperature of T_∞ . The thermal boundary layer is generally not coincident with the velocity boundary layer, although it is certainly dependent on it. If the fluid has high thermal conductivity, it will be thicker than the velocity boundary layer, and if conductivity is low, it will be thinner than the velocity boundary layer.

Dimensionless Parameters

The dimensionless parameters can be thought of as measures of the relative importance of certain aspects of the flow. Some dimensionless parameters related to our study are discussed below:

Grashof number *Gr*

The flow regime in free convection is governed by the dimensionless Grashof number, which represent the ratio of the buoyancy force to the viscous forces acting on the fluid, and is defined as

$$Gr = \frac{g\beta L^3 \left(T_w - T_\infty\right)}{\nu^2}$$

Where, g is the acceleration due to gravity, β is the volumetric thermal expansion coefficient, T_w is the wall temperature, T_∞ is the ambient temperature, L is the characteristic length and ν is the kinematics viscosity. The Grashof number *Gr* plays same role in free convection as the Reynolds number *Re* plays in forced convection. As such, the Grashof number provides the main criterion in determining whether the fluid flow is laminar or turbulent in free convection. For vertical plates, the critical value of the Grashof number is observed to be about 10^9. Therefore, the flow regime on a vertical plate becomes turbulent at Grashof numbers greater than 10^9.

Prandtl Number *Pr*

The Prandtl number is a measure of the relative importance of heat conduction and viscosity of a fluid and is defined as $Pr = \frac{\mu C_p}{\kappa}$

where C_p is the specific heat of the fluid at constant pressure, and *k* is the coefficient of thermal conductivity of the fluid. The Prandtl number may also be written as follows:

$$Pr = \frac{\mu/\rho}{\kappa/C_p\rho} = \frac{\nu}{\kappa/C_p\rho} = \text{(Kinematics viscosity)/ (thermal diffusivity)}$$

The value of ν shows the effect of viscosity of a fluid. If other things are the same, the smaller the value of ν, the narrower will be the region affected by viscosity. This region is known as the boundary-layer region when ν is very small. While ν shows the momentum diffusivity due to viscosity effect, $\kappa/C_p\rho$ shows the thermal diffusivity

due to heat conduction. The smaller value of $\kappa / C_p \rho$, the narrower will be the region affected by heat conduction. This region is known as thermal boundary layer when $\kappa / C_p \rho$ is very small. Thus the Prandtl number shows the relative importance of heat conduction and viscosity of a fluid. Since for a gas the Prandtl number is of the order of unity, whenever the effect of viscosity is considered we must simultaneously take into account of the influence of the thermal conductivity of the gas. The Prandtl numbers of fluids range from less than 0.01 for liquid metals to more than 100,000 for heavy oils. Note that the Prandtl number is in the order of 7 for water. The Prandtl numbers of gases are about 1, which indicates that both momentum and heat dissipate through the fluid at about the same rate. Consequently the thermal boundary layer is much thicker for liquid metals and much thinner for oils relative to the velocity boundary layer.

Nusselt Number *Nu*

The Nusselt number represents the enhancement of heat transfer through a fluid layer as a result of convection relative to conduction across the same fluid layer, and is defined as

$Nu = hL / \kappa$

where κ is the thermal conductivity of the fluid, h is the heat transfer coefficient and L is the characteristics length. The Nusselt number is named after Wilhelm Nusselt, who made significant contributions to convective heat transfer in the first half of the twentieth century, and it is viewed as the dimensionless convection heat transfer coefficient. The larger Nusselt number indicates a large temperature gradient at the surface and hence, high heat transfer by convection. A Nusselt number of $Nu = 1$, for a fluid layer represents heat transfer across the layer by pure conduction. To understand the physical significance of the Nusselt number, consider the following daily life problems. We remedy to forced convection whenever we want to increase the rate of heat transfer from a hot object. In free convection flow velocities are produced by the buoyancy forces hence there are no externally induced flow velocities.

1.3 Main Objectives of the Work

This research is to investigate the effects of temperature dependent thermal conductivity on MHD conjugate free convection flow with heat generation and pressure work along a vertical flat plate.

Solutions are obtained and analyzed in terms of fluid properties like the skin friction coefficient, surface temperature distribution along the plate and the velocity profiles and temperature distributions over the whole boundary layer for a selection of parameters set consisting of the Prandtl number Pr, magnetic parameter M, thermal conductivity variation parameter γ, heat generation parameter Q and pressure work parameter ε.

The major objectives of this study are:

1. To study the effects of magnetic parameter M on velocity and temperature profiles, skin friction coefficient and surface temperature distribution.
2. To investigate the effects of Prandtl number Pr on velocity and temperature profiles, skin friction coefficient and surface temperature distribution.
3. To analyze the effects of thermal conductivity variation γ on velocity and temperature profiles, skin friction coefficient and surface temperature distribution.
4. To investigate the effects of heat generation parameter Q on velocity and temperature profiles, skin friction coefficient and surface temperature profiles.
5. To study the effects of pressure work parameter ε on velocity and temperature profiles, skin friction coefficient and surface temperature profiles.
6. To compare the present results with other published works.

1.4 Literature Survey

The study of the flow of electrically conducting fluid like mercury in presence of magnetic field and the effect of temperature dependent thermal conductivity on a vertical flat plate with heat generation and pressure work problems are important from the technical point of view and such types of problems have received much attention by many researchers. Experimental and theoretical works on MHD free and forced convection flow have been done extensively but a few works were given over the conjugate effects of convection and conduction problems. The combined free and forced convection flow about inclined surfaces in porous media were studied by Chen (1977). The combined forced and free convection in boundary layer flow of a micro polar fluid over a horizontal plate was investigated by Hassanien (1977); Similarity solutions were acquired in his work for the case of wall temperature, which is inversely proportional to the square root of the distance from the leading edge.

The case of a heated isothermal horizontal surface with transpiration was discussed in some detail by Clarke and Riley (1975, 1976). Takhar and Soundalgekar (1980) studied the dissipation effects on MHD free convection flow past a semi-infinite vertical plate. The effect of axial heat conduction in a vertical flat plate on free convection heat transfer was studied by Miyamoto et al. (1980). A transformation of the boundary layer equations for free convection past a vertical plate with arbitrary blowing and wall temperature variations was studied by Vidhanayagam et al. (1980). Moreover, Raptis and Kafoussias (1982) investigated the problem of MHD free convection flow and mass transfer through a porous medium bounded by an infinite vertical porous plate with constant heat flux. Pozzi and Lupo (1988) investigated the coupling of conduction with laminar convection along a flat plate. Lin and Yu (1988) studied further detail discussion of a heated isothermal horizontal surface with transpiration.

The problem of the free convection boundary layer on a vertical plate with prescribed surface heat flux was studied by Merkin and Mahmood (1990). Hossain (1992) analyzed the viscous and joule heating effects on MHD free convection flow with variable plate temperature. Pop et al. (1995) then extended the analysis to conjugate mixed convection on a vertical surface in porous medium. Moreover, the thermal interaction between laminar film condensation and forced convection along a conducting wall was investigated by Chen Chang (1996). Merkin and Pop (1996) analyzed the Conjugate free convection on a vertical surface. Hossain et al. (1997) studied the force and free

convection boundary layer flow along a vertical porous plate in presence of magnetic field. Also Hossain et al. (1998) investigated the heat transfer response of MHD free convection flow along a vertical plate to surface temperature oscillation. Shu and Pop (1999) analyzed the thermal interaction between free convection and forced convection along a vertical conducting wall. Al-Khawaja et al. (1999) also studied MHD mixed convection flow.

MHD free convection flow of visco-elastic fluid past an infinite porous plate was investigated by Chowdhury M. K. and Islam M. N. (2000). Elbashbeshy (2000) also discussed the effect of free convection flow with variable viscosity and thermal diffusivity along a vertical plate in the presence of magnetic field. Khan Z. I. (2002) investigated the conjugate effect of conduction and convection with natural convection flow from a vertical flat plate and in an inclined square cavity. Ahmad and Zaidi (2004) investigated the magnetic effect on over back convection through vertical stratum. Chen (2006) analyzed a numerical simulation of micropolar fluid flows along a flat plate with wall conduction and buoyancy effects. Mamun et al. (2005) has studied natural convection flow from an isothermal sphere with temperature dependent thermal conductivity. Alim et al. (2007) investigated the Joule heating effect on the coupling of conduction with MHD free convection flow from a vertical flat plate. Mamun et al. (2008) analyzed conjugate heat transfer for a vertical flat plate with heat generation effect. Rahman et al. (2008) investigated the effects of temperature dependent thermal conductivity on MHD free convection flow along a vertical flat plate with heat conduction.

In all the aforementioned analyses the effects of temperature dependent thermal conductivity with heat generation and pressure work have not been considered. In the present work, the effects of temperature dependent thermal conductivity on the coupling of conduction in the presence of heat generation and pressure work with MHD free convection flow along a vertical flat plate have been investigated. The results have been obtained for different values of relevant physical parameters. The governing partial differential equations are reduced to locally non-similarity partial differential forms by adopting appropriate transformations. The transformed boundary layer equations are solved numerically using implicit finite difference method together with H.B. Keller (1978) box technique that later used by T. Cebeci and P. Bradshaw (1984).

In chapter 2, the effects of the temperature dependent thermal conductivity on MHD free convection flow along a vertical flat plate with heat generation and conduction have been described. The non–dimensional boundary layer equations have been solved by using implicit finite difference methods by H.B Keller (1978) that later used by T. Cebeci and P. Bradshaw (1984) .The Velocity profiles, temperature profiles, skin friction coefficient and surface temperature have been presented for various values of the magnetic parameter M, Prandtl number Pr, thermal conductivity variation parameter γ and heat generation parameter Q.

The comparisons of the present numerical results of the skin friction co-efficient and the surface temperature profile with those obtained by Pozzi and Lupo (1988) and Merkin and Pop (1996) are presented.

In chapter 3, Conjugate effects of temperature dependent thermal conductivity on MHD free convection flow along a vertical flat plate with heat generation and pressure work have been analyzed. Numerical results of the velocity, temperature, skin friction coefficient and surface temperature for different values of the magnetic parameter M, Prandtl number Pr, thermal conductivity variation parameter γ, heat generation parameter Q and pressure work parameter ε have been presented graphically.

The comparisons of the present numerical results of the skin friction co-efficient and the surface temperature profile with those obtained by Pozzi and Lupo (1988) and Merkin and Pop (1996) are presented.

Chapter 2

Effects of Temperature Dependent Thermal Conductivity on Magnetohydrodynamic Free Convection Flow along a Vertical Flat Plate with Heat Generation

2.1 Introduction

The effects of the temperature dependent thermal conductivity on MHD free convection flow along a vertical flat plate with heat generation and conduction have been described in this chapter. The governing boundary layer equations are transformed into a non dimensional form and the resulting non linear system of partial differential equations are reduce to local non similarity equations which are solved numerically by very efficient implicit finite difference method together with Keller box technique. Numerically results are presented by velocity, temperature, skin friction coefficient and surface temperature profiles for magnetic parameter M, thermal conductivity variation parameter γ, Prandtl number Pr and heat generation parameter Q. In the following section detailed derivations of the governing equations for the flow and the method of solutions along with the results and discussions are presented.

2.2 Governing equations of the flow

In the presence of heat generation with temperature dependent thermal conductivity, the free convection flow of an electrically conducting, viscous and incompressible fluid along a vertical flat plate of length l and thickness b has been investigated. Over the work it is assumed that the temperature at the outside surface is maintained at a constant temperature T_b, where $T_b > T_\infty$, the ambient temperature of the fluid, g is the acceleration due to gravity. A uniform magnetic field of strength H_0 is imposed along the $\bar{y}$-axis (Figure 2).

Under the usual Boussinesq approximation, $\rho = \rho_\infty[1-\beta(T_b - T_\infty)]$, where ρ_∞ and T_∞ are the density and temperature respectively outside the boundary layer, β is the coefficient of thermal expansion.

The continuity, momentum and energy equations of such flow can be written as:

$$\frac{\partial \bar{u}}{\partial \bar{x}} + \frac{\partial \bar{v}}{\partial \bar{y}} = 0 \tag{2.1}$$

$$\bar{u}\frac{\partial \bar{u}}{\partial \bar{x}} + \bar{v}\frac{\partial \bar{u}}{\partial \bar{y}} = \nu \frac{\partial^2 \bar{u}}{\partial \bar{y}^2} + g\beta(T_f - T_\infty) - \frac{\sigma H_0^2\, \bar{u}}{\rho} \tag{2.2}$$

$$\bar{u}\frac{\partial T_f}{\partial \bar{x}} + \bar{v}\frac{\partial T_f}{\partial \bar{y}} = \frac{1}{\rho C_p}\frac{\partial}{\partial \bar{y}}(\kappa_f \frac{\partial T_f}{\partial \bar{y}}) + \frac{Q_0}{\rho C_p}\left(T_f - T_\infty\right) \tag{2.3}$$

Consider the temperature dependent thermal conductivity, which is proposed by Charraudeau (1975), as follows

$$\kappa_f = \kappa_\infty[1 + \delta(T_f - T_\infty)] \tag{2.4}$$

where, κ_∞ is the thermal conductivity of the ambient fluid and δ is defined as follows

$$\delta = \frac{1}{\kappa_f}\left(\frac{\partial \kappa}{\partial T}\right)_f \tag{2.5}$$

The appropriate boundary conditions to be satisfied by the above equations are (Hossain 1992, Chang 2006, Merkin & Pop 1996)

$$\left.\begin{aligned} &\bar{u} = 0, \qquad \bar{v} = 0 \\ &T_f = T(\bar{x},0), \quad \frac{\partial T_f}{\partial \bar{y}} = \frac{\kappa_s}{b\kappa_f}(T_f - T_b) \end{aligned}\right\} \quad on \quad \bar{y} = 0,\ \bar{x} > 0$$
$$\bar{u} \to 0,\ T_f \to T_\infty \ \ as \quad \bar{y} \to \infty, \quad \bar{x} > 0 \tag{2.6}$$

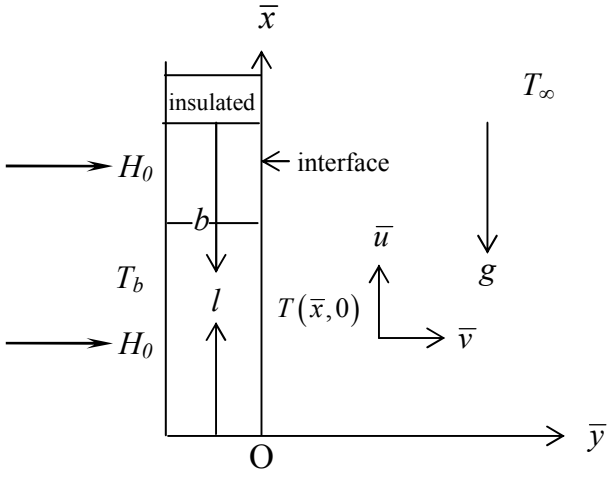

Figure 2: Physical model and coordinate system

Observed that the equations (2.2) and (2.3) together with the boundary conditions (2.6) are non-linear partial differential equations. In the following sections the solution methods of these equations are discussed in details

2.3 Transformation of the governing equations

Equations (2.1) to (2.3) will be non-dimensionalized by using the following dimensionless variables

$$x=\frac{\bar{x}}{L},\ y=\frac{\bar{y}}{L}Gr^{\frac{1}{4}},\ u=\frac{\bar{u}L}{\nu}Gr^{-\frac{1}{2}},\ v=\frac{\bar{v}L}{\nu}Gr^{-\frac{1}{4}},\ \theta=\frac{T_f-T_\infty}{T_b-T_\infty},$$
$$Gr=\frac{g\beta L^3(T_b-T_\infty)}{\nu^2} \tag{2.7}$$

where $L=\frac{\nu^{2/3}}{g^{1/3}}$ is reference length , Gr is the Grashof number, θ is the non dimensional temperature, $\nu=\mu/\rho$ is kinematic viscosity. As the problem of free convection, its parabolic character has no characteristic length, L is the intrinsic properties of the system. It is along the y-direction has been modified by a factor $Gr^{1/4}$ in order to eliminate this quantity from the dimensionless equations and boundary conditions.

Substituting the relations (2.7) into the equations (2.1) to (2.3) then the following non-dimensional equations

$$\frac{\partial u}{\partial x}+\frac{\partial v}{\partial y}=0 \tag{2.8}$$

$$u\frac{\partial u}{\partial x}+v\frac{\partial u}{\partial y}+Mu=\frac{\partial^2 u}{\partial y^2}+\theta \tag{2.9}$$

$$u\frac{\partial \theta}{\partial x}+v\frac{\partial \theta}{\partial y}=\frac{1}{\Pr}(1+\gamma\theta)\frac{\partial^2\theta}{\partial y^2}+\frac{\gamma}{\Pr}\left(\frac{\partial\theta}{\partial y}\right)^2+Q\theta \tag{2.10}$$

where, $M=\frac{\sigma H_0{}^2L^2}{\mu\, Gr^{1/2}}$ is the dimensionless magnetic parameter, $\Pr=\frac{\mu\, C_p}{\kappa_\infty}$ is the Prandtl number, $\gamma=\delta(T_b-T_\infty)$ is the dimensionless thermal conductivity variation

parameter and $Q = \dfrac{Q_0 L^2}{\mu C_p Gr^{1/2}}$ is the dimensionless heat generation parameter . The corresponding boundary conditions (2.6) then take the following form

$$\begin{aligned} &u = 0, v = 0, \ \theta - 1 = (1+\gamma\theta)\ p\frac{\partial\theta}{\partial y} \quad on \ \ y = 0, x > 0 \\ &u \to 0, \theta \to 0 \quad as \ \ y \to \infty, x > 0 \end{aligned} \tag{2.11}$$

where, $p = \left(\dfrac{\kappa_\infty\, b}{\kappa_s L}\right) Gr^{\frac{1}{4}}$ is the conjugate conduction parameter. In actual fact, magnitude of O(p) depends on b/L and $Gr^{1/4}$ being the order of unity. L is small, the term b/L becomes greater than one. For air, $\dfrac{\kappa_\infty}{\kappa_s}$ attains very small values if the plate is highly conductive and reaches the order of 0.1 for materials such as glass. Therefore in different cases p is different but not always a small number. In the present investigation we have considered p = 1 which is accepted for b/L of $O(\dfrac{\kappa_\infty}{\kappa_s})$.

To solve the equations (2.9) and (2.10) subject to the boundary conditions (2.11) the following transformations are introduced (Merkin & Pop 1996):

$$\begin{aligned} \psi &= x^{\frac{4}{5}}(1+x)^{-\frac{1}{20}} f(x,\eta) \\ \eta &= y\, x^{-\frac{1}{5}}(1+x)^{-\frac{1}{20}} \\ \theta &= x^{\frac{1}{5}}(1+x)^{-\frac{1}{5}} h(x,\eta) \end{aligned} \tag{2.12}$$

here η is the similarity variable and ψ is the non-dimensional stream function which satisfies the continuity equation and is related to the velocity components in the usual way as $u = \dfrac{\partial\psi}{\partial y}$ and $v = -\dfrac{\partial\psi}{\partial x}$. Moreover, $h(x,\eta)$ represents the non-dimensional temperature. The momentum and energy equations (equations (2.9) and (2.10) respectively) are transformed for the new co-ordinate system. At first, the velocity components are expressed in terms of the new variables for this transformation. Thus the following equations

$$f''' + \frac{16+15x}{20(1+x)} f f'' - \frac{6+5x}{10(1+x)} f'^2 - M x^{\frac{2}{5}} (1+x)^{\frac{1}{10}} f' + h = x\left(f' \frac{\partial f'}{\partial x} - f'' \frac{\partial f}{\partial x} \right) \tag{2.13}$$

$$\frac{1}{\Pr} h'' + \frac{\gamma}{\Pr} \left(\frac{x}{1+x} \right)^{\frac{1}{5}} h h'' + \frac{\gamma}{\Pr} \left(\frac{x}{1+x} \right)^{\frac{1}{5}} h'^2 + \frac{16+15x}{20(1+x)} f h' + Q x^{2/5} (1+x)^{1/10} h - \frac{1}{5(1+x)} f' h = x\left(f' \frac{\partial h}{\partial x} - h' \frac{\partial f}{\partial x} \right) \tag{2.14}$$

where, prime denotes partial differentiation with respect to η. The boundary conditions as mentioned in equation (2.11) then take the following form:

$$f(x,0) = f'(x,0) = 0$$
$$h'(x,0) = \frac{x^{\frac{1}{5}} (1+x)^{-\frac{1}{5}} h(x,0) - 1}{(1+x)^{-\frac{1}{4}} + \gamma x^{\frac{1}{5}} (1+x)^{-\frac{9}{20}} h(x,0)} \tag{2.15}$$
$$f'(x,\infty) \to 0, \quad h'(x,\infty) \to 0$$

The set of equations (2.13) and (2.14) together with the boundary conditions (2.15) are solved by applying implicit finite difference method with Keller (1978) box scheme.

A good description of this method and its application to the boundary layer flow problems are given in the book by T. Cebeci and P. Bradshaw (1984). From the process of numerical computation, in practical point of view, it is important to calculate the values of the surface shear stress in terms of the skin friction coefficient. This can be written in the non-dimensional form as (Mamun et al. 2005)

$$C_f = \frac{Gr^{-\frac{3}{4}} L^2}{\mu \nu} \tau_w \tag{2.16}$$

where, $\tau_w [= \mu(\partial \bar{u} / \partial \bar{y})_{\bar{y}=0}]$ is the shearing stress. Using the new variables described in (2.7), the local skin friction co-efficient can be written as

$$C_{fx} = x^{\frac{2}{5}} (1+x)^{-\frac{3}{20}} f''(x,0) \tag{2.17}$$

The numerical values of the surface temperature distribution are obtained from the relation

$$\theta(x,0) = x^{\frac{1}{5}} (1+x)^{-\frac{1}{5}} h(x,0) \tag{2.18}$$

2.4 Results and Discussions

Here we have considered the thermal conductivity of the fluid is proportional to the linear function of temperature that means if the temperature of the fluid increases, the conductivity of the fluid increases. The thermal conductivity of air is 0.009246 $W.m^{-10}.K^{-1}$, 0.01809 $W.m^{-10}.K^{-1}$, 0.02624 $W.m^{-10}.K^{-1}$ and 0.03365 $W.m^{-10}.K^{-1}$ at 100^0 K, 200^0 K, 300^0 K and 400^0 K temperature respectively. (See T. Cebeci and P. Bradshaw, (1984)). Solutions are obtained for the values of Prandle number Pr = 0.72, 1.00, 1.44, 1.74 and for a wide range of the magnetic parameter M = 0.10, 0.50, 0.90, 1.40, thermal conductivity γ = 0.05, 0.15, 0.30, 0.50 and heat generation parameter Q =0.01, 0.05, 0.10, 0.15. Detailed numerical results of the velocity, temperature, skin friction coefficient and surface temperature profiles for different values of magnetic parameter M, Prandtl number Pr, thermal conductivity variation parameter γ and heat generation parameter Q are presented graphically in figure 2.1 to figure 2.16.

For a particular parameter the velocity increases and attains at maximum point then decreases and finally approaches to zero along η direction.

Figures 2.1 and 2.2 display the velocity and the temperature profiles for the different values of the magnetic parameter M. It is observed that the velocity decreases for the increasing value of the magnetic parameter M between $0 \leq \eta \leq 4.59386$ and then increases with very small difference and finally approaches to zero along η direction. This is due to the fact that the velocity decreases rapidly for the small value of M comparatively, for the large value of M. The temperature increases with the increasing value of the magnetic parameter M. This phenomenon can easily be understood from the fact that the interaction of the magnetic field and the moving electric charge carried by the flowing fluid induces a force, which tends to oppose the fluid motion and increases the temperature. The maximum values of the velocity are recorded as 0.49573, 0.41922, 0.36244 and 0.31081 for M = 0.10, 0.50, 0.90 and 1.40 respectively which occur at η = 1.42791 for 1^{st} and 2^{nd} maximum values and at η = 1.38267 for 3^{rd} and 4^{th} maximum values. It is found that the velocity decreases by 37.30% as the value of the magnetic parameter M increases from 0.10 to 1.40. It also observed that the temperature at the interface varies due to the conduction within the plate.

Figures 2.3 and 2.4 indicate the effects of the Prandtl number Pr on the velocity and temperature profiles. From figure 2.3 it is observed that the velocity decreases as well as

its position moves toward the interface with the increasing value of the Prandtl number *Pr*. The overall temperature also shift downwards with the increasing value of *Pr* as observed in figure 2.4. These are expected, since the viscosity increases and the thermal conductivity decreases with the increasing value of Pr. The maximum values of the velocity are 0.49573, 0.44728, 0.39726 and 0.37293 for *Pr* = 0.72, 1.00, 1.44 and 1.74 respectively which occur at $\eta = 1.42791$ for 1st maximum value, at $\eta = 1.38267$ for 2nd maximum value, at $\eta = 1.29502$ for 3rd maximum value and at $\eta = 1.25254$ for last maximum value. Here it is depicted that the velocity decreases by 24.77% as the value of *Pr* increases from 0.72 to 1.74.

The effects of the thermal conductivity variation parameter γ on the velocity and the temperature within the boundary layer are shown in figures 2.5 and 2.6 respectively. It is seen from figures 2.5 and 2.6 that the velocity and the temperature increase within the boundary layer with the increasing value of γ. This is due to the fact that for increasing value of γ, the temperature of the fluid within the boundary layer increases. It means that the velocity boundary layer and the thermal boundary layer thickness increase for large values of γ. The maximum values of the velocity are 0.49346, 0.49793, 0.51413 and 0.51161 for $\gamma = 0.05$, 0.15, 0.30 and 0.50, respectively which occur at $\eta = 1.42791$ for 1st, 2nd and 3rd maximum values and at $\eta = 1.38267$ for 4th maximum value. It is observed that the velocity increases by 3.68% when the value of γ increases from 0.05 to 0.50. This is to be expected because the higher value of the thermal conductivity variation parameter accelerates the fluid flow and increases the temperature.

The effects of heat generation parameter *Q* on the velocity and the temperature within the boundary layer are shown in figures 2.7 and 2.8. It is seen from figures 2.7 and 2.8 that the velocity and the temperature increase within the boundary layer with the increasing value of the heat generation parameter *Q*. These are expected, since the increased value of Q means that the more heat is produced and it creates a layer of hot fluid near the surface, eventually that heat increases the fluid motion. The maximum values of the velocity are 0.46359, 0.47763, 0.49573, and 0.51442 for *Q* =0.01, 0.05 0.10 and 0.15 respectively which each occurs at $\eta = 1.42791$. Here it is observed that the velocity increases by 10.96% as the value of *Q* increases from 0.01 to 0.15.

It can easily be seen that the local skin friction coefficient decreases and the surface temperature increases for the increasing value of the magnetic parameter *M* in figures 2.9

and 2.10. This phenomenon can easily be understood from the fact that the magnetic parameter M increases the Lorentz force which opposes the flow, therefore, it decreases the velocity gradient and hence the local skin friction coefficient C_{fx} decreases. Again figure 2.10 shows that the surface temperature $\theta(x,0)$ increases due to the increased value of the magnetic parameter M. It can also be seen that the surface temperature increases along the upward direction of the plate for a particular value of M. This is due to the fact that the magnetic field acts against the flow and reduces the skin friction and produces the temperature at the interface. So the magnetic field decreases the temperature gradient at the wall and increases the temperature in the flow region.

Figures 2.11 and 2.12 deal with the effects of Prandtl number Pr on the local skin friction coefficient and the surface temperature distribution. It can be observed from figure 2.11 that the skin friction coefficient increases monotonically for a particular value of Pr. It can also be noted that the skin friction coefficient decreases for the increasing value of Pr. From figure 2.12, it can be seen that the surface temperature decreases owing to the increasing value of the Prandtl number.

Figures 2.13 and 2.14 illustrate the effects of the thermal conductivity variation parameter γ on the local skin friction coefficient and the surface temperature distribution. From figure 2.13, it is seen that the skin friction coefficient increases monotonically along the upward direction of the plate for a particular value of γ. It is also seen that the skin friction factor increases for the increasing value of γ. From figure 2.14, it is seen that the surface temperature increases along the positive x-direction for the increasing value of γ. This is to be expected because the higher value for the thermal conductivity variation parameter accelerates the fluid flow and increases the temperature as mentioned in figure 2.5 and 2.6 respectively.

The variation of the local skin friction coefficient and the surface temperature distribution for different values of the heat generation parameter Q are illustrated in figures 2.15 and 2.16. From the figures it can be seen that the increased value of the heat generation parameter Q leads to an increased in the local skin friction coefficient and the surface temperature. These are expected, since the heat generation mechanism creates a layer of hot fluid near the surface and finally the resultant temperature of the fluid exceeds the surface temperature.

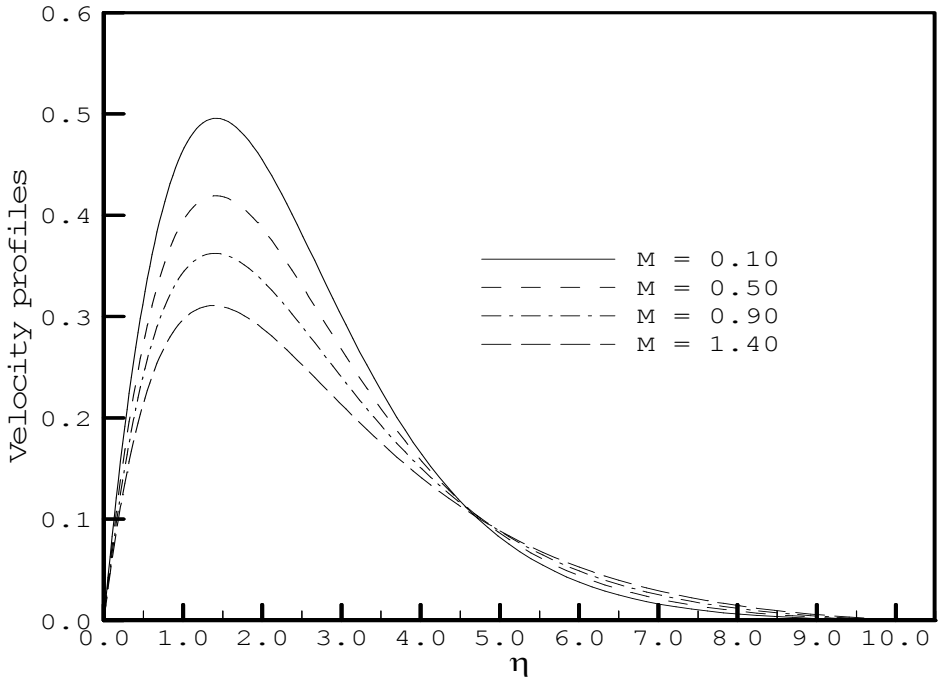

Figure 2.1: Variation of velocity profiles for different value of M with $Pr = 0.72$, $\gamma = 0.10$ and $Q = 0.10$

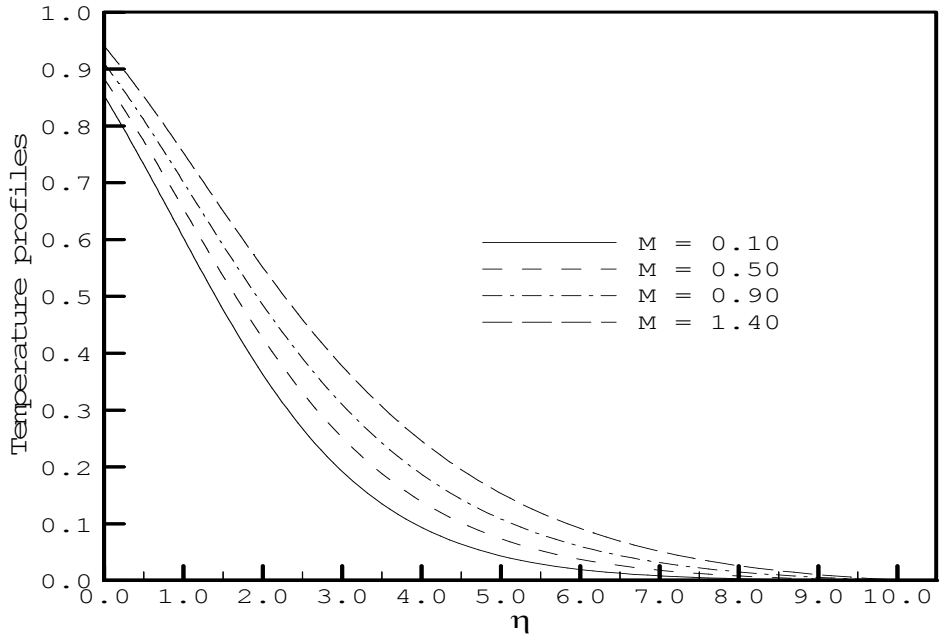

Figure 2.2: Variation of Temperature profiles for different value of M with $Pr = 0.72$, $\gamma = 0.10$ and $Q = 0.10$

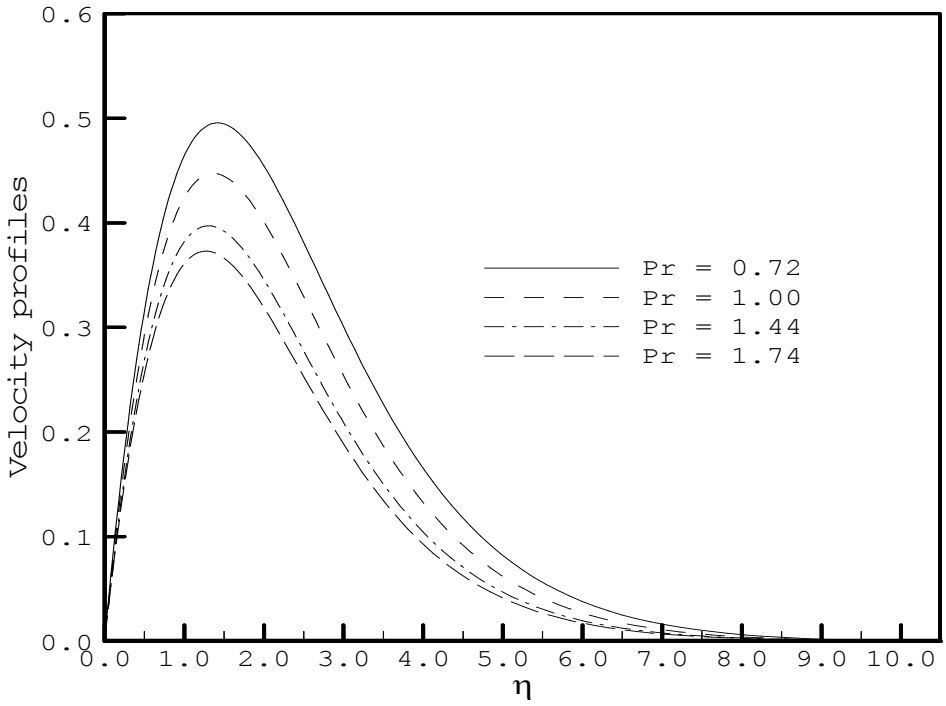

Figure 2.3: Variation of velocity profiles for different value of *Pr* with $M = 0.10$, $\gamma = 0.10$ and $Q = 0.10$

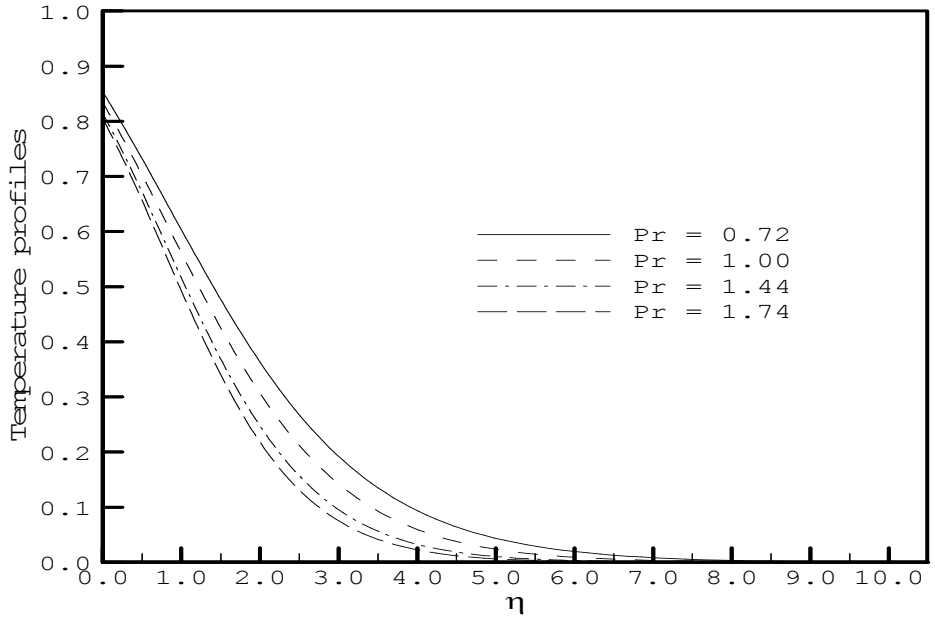

Figure 2.4: Variation of Temperature profiles for different value of *Pr* with $M = 0.10$, $\gamma = 0.10$ and $Q = 0.10$

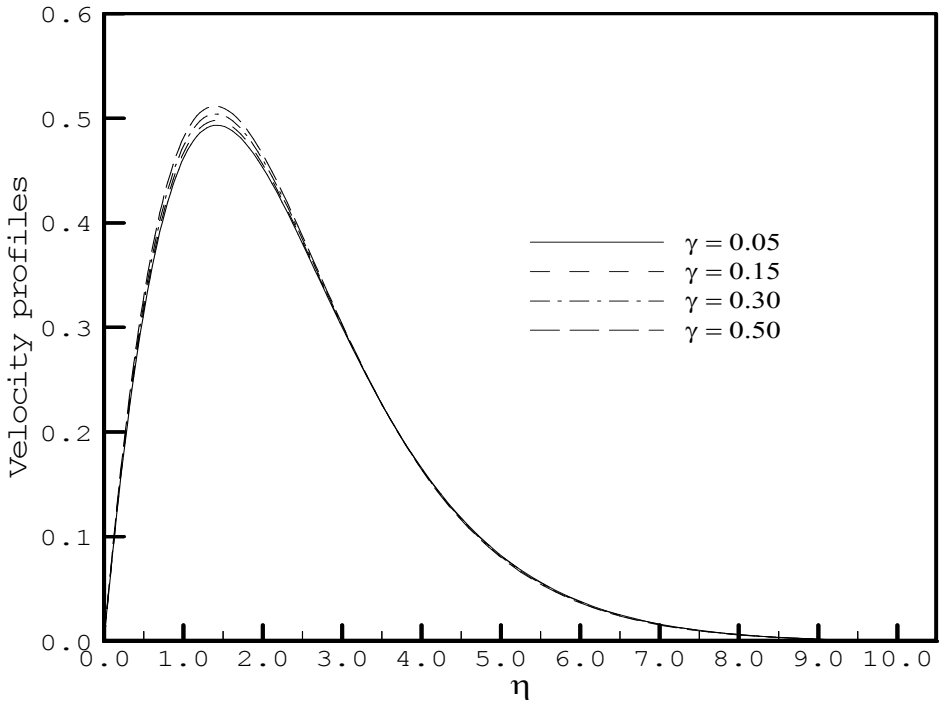

Figure 2.5: Variation of velocity profiles for different value of γ with $M = 0.10$, $Pr = 0.72$ and $Q = 0.10$

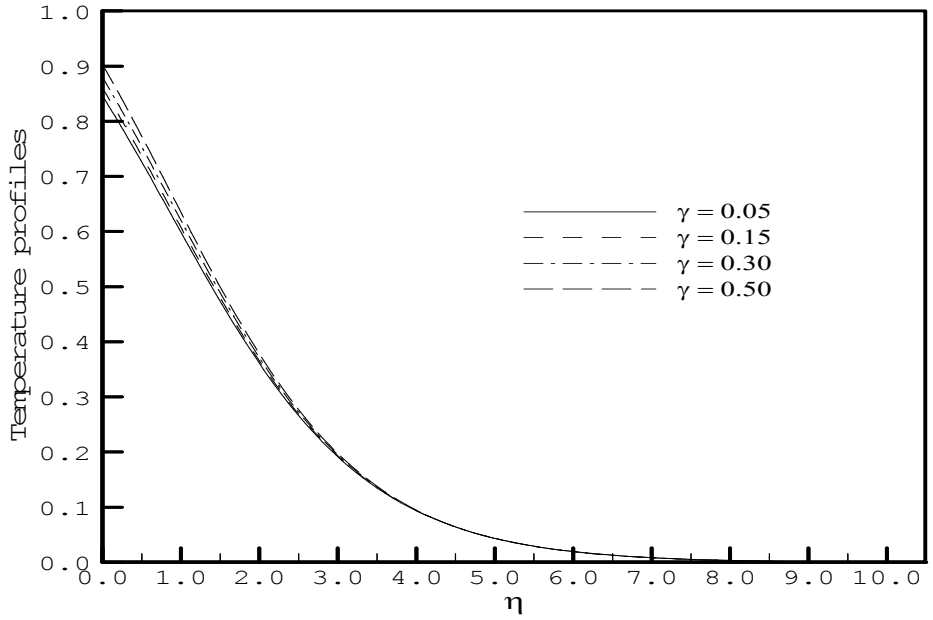

Figure 2.6: Variation of Temperature profiles for different value of γ with $M = 0.10$, $Pr = 0.72$ and $Q = 0.10$

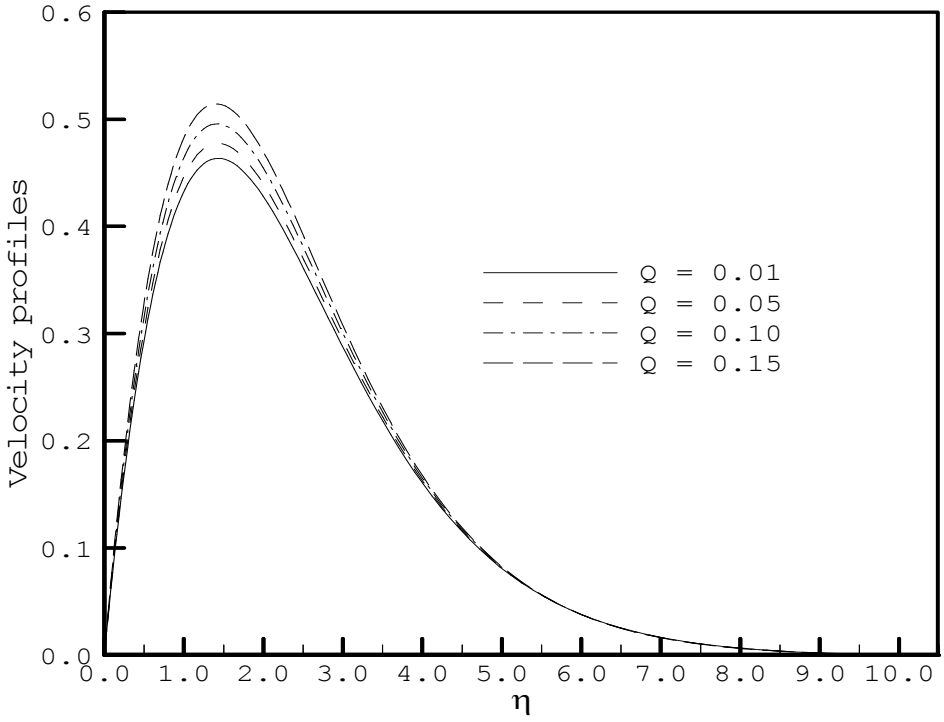

Figure 2.7: Variation of velocity profiles for different value of Q with $M = 0.10$, $Pr = 0.72$ and $\gamma = 0.10$

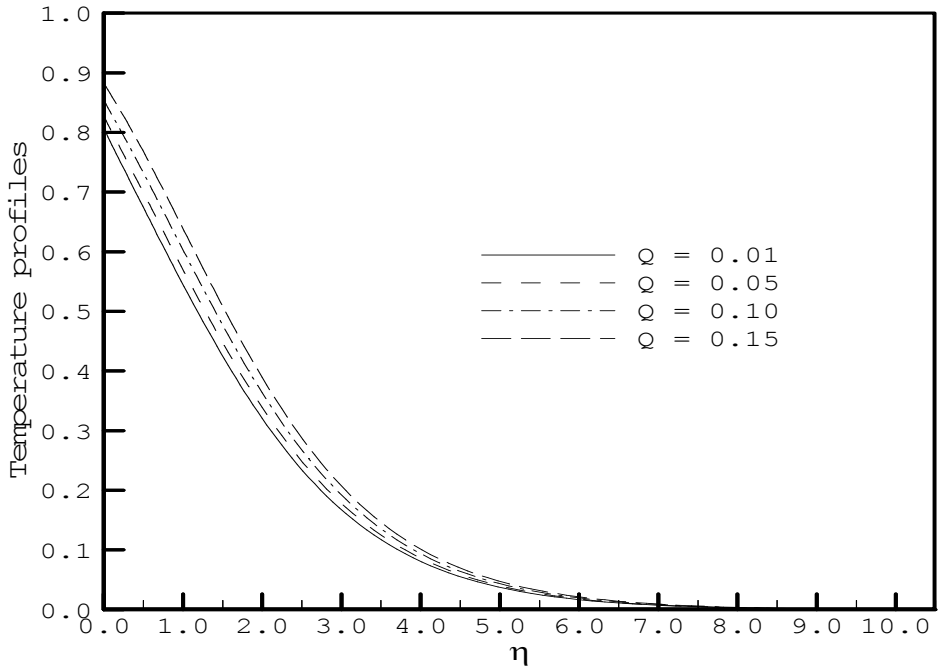

Figure 2.8: Variation of Temperature profiles for different value of Q with $M = 0.10$, Pr = 0.72 and $\gamma = 0.10$

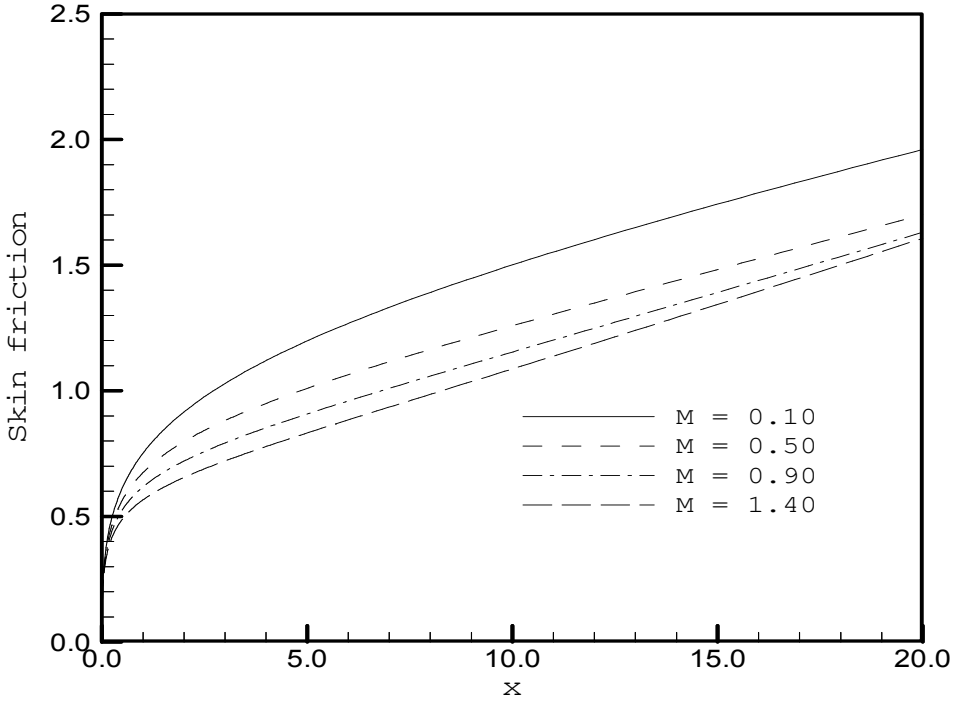

Figure 2.9: Variation of skin friction coefficient for different value of M with $Pr = 0.72$, $\gamma = 0.10$ and $Q = 0.10$

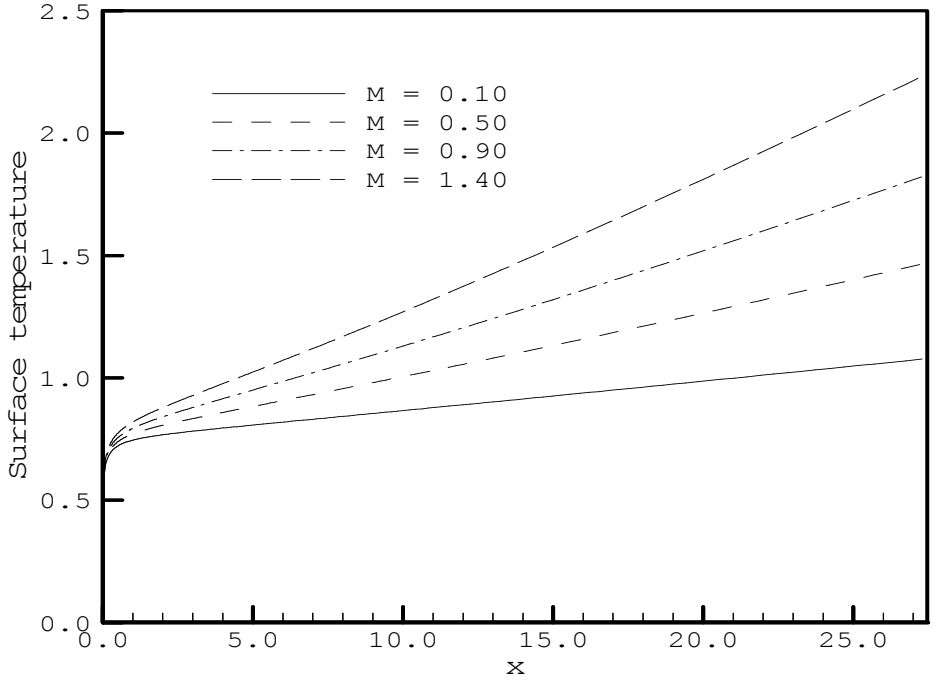

Figure 2.10: Variation of surface temperature profiles for different value of M with $Pr = 0.72$, $\gamma = 0.10$ and $Q = 0.10$

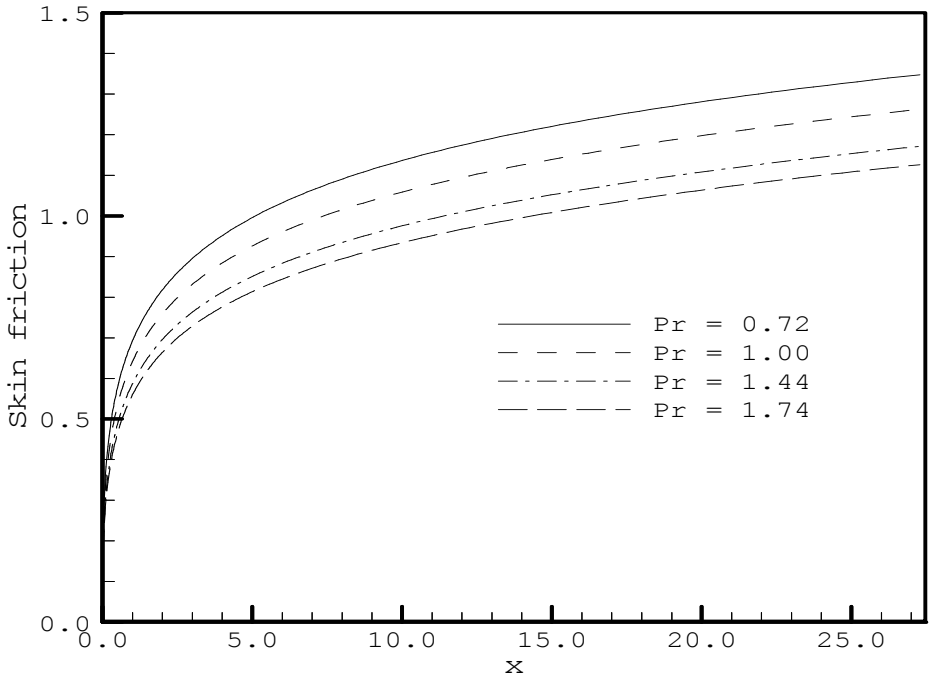

Figure 2.11: Variation of skin friction coefficient for different value of *Pr* with $M = 0.10$, $\gamma = 0.01$ and $Q = 0.01$

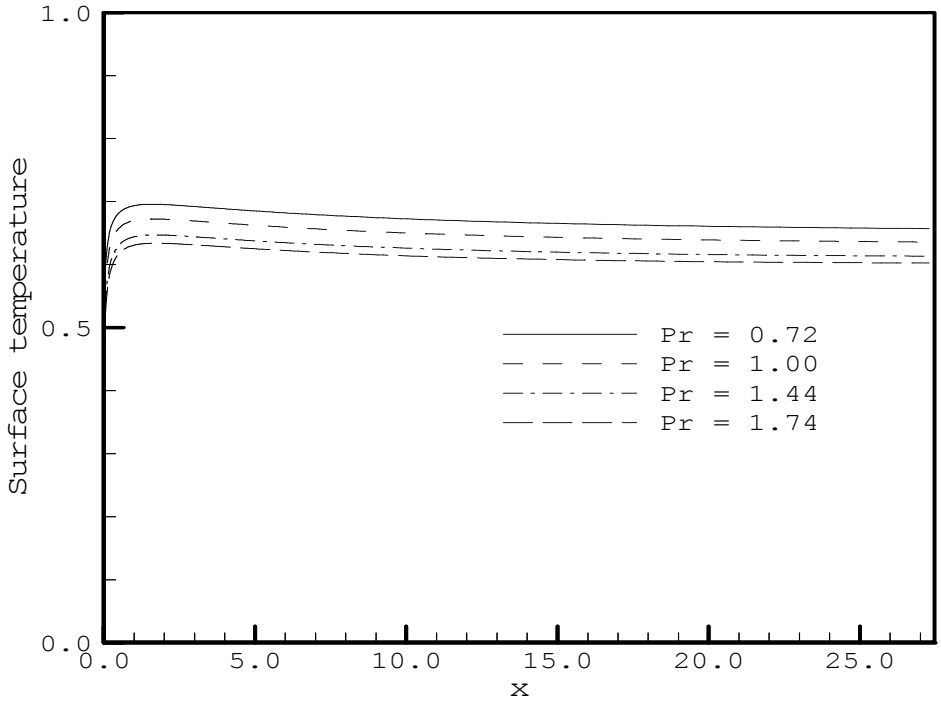

Figure 2.12: Variation of surface temperature profiles for different value of *Pr* with $M = 0.10$, $\gamma = 0.01$ and $Q = 0.01$

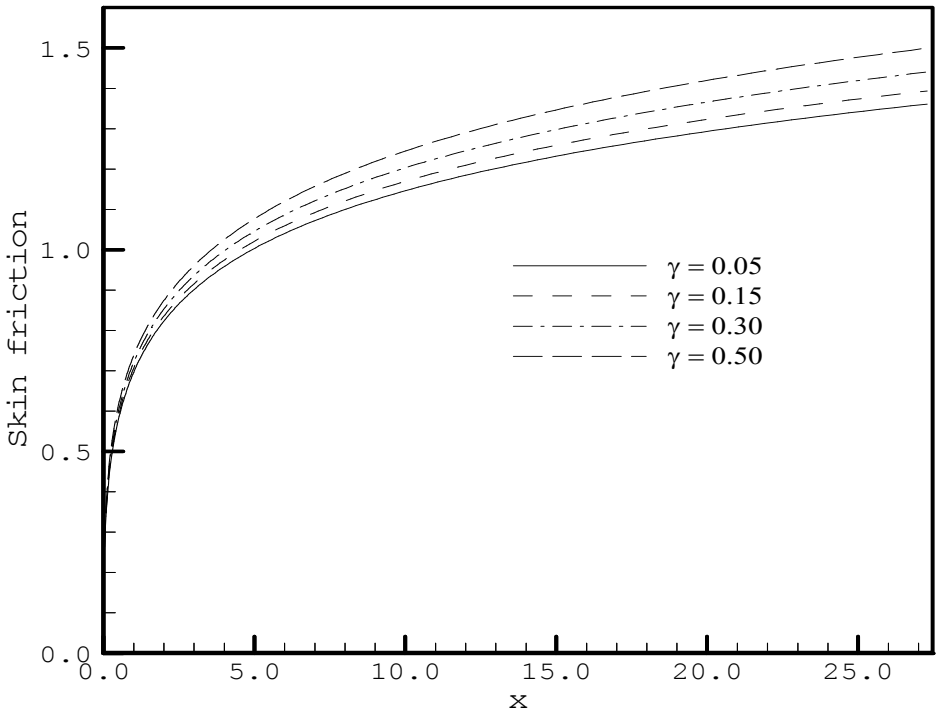

Figure 2.13: Variation of skin friction coefficient for different value of γ with $M = 0.10$, $Pr = 0.72$ and $Q = 0.01$

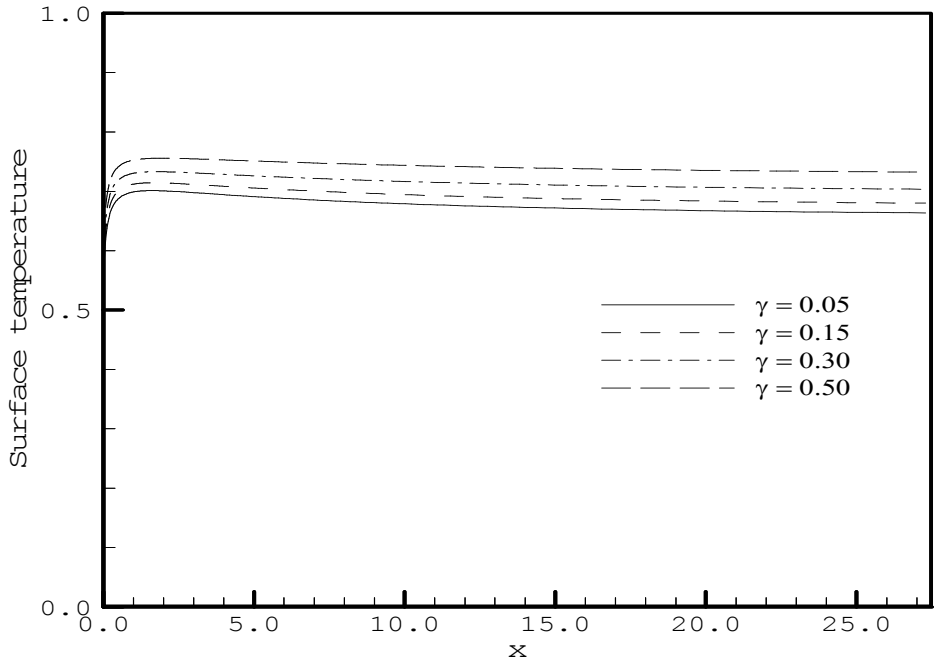

Figure 2.14: Variation of surface temperature profiles for different value of γ with $M = 0.10$, $Pr = 0.72$ and $Q = 0.01$

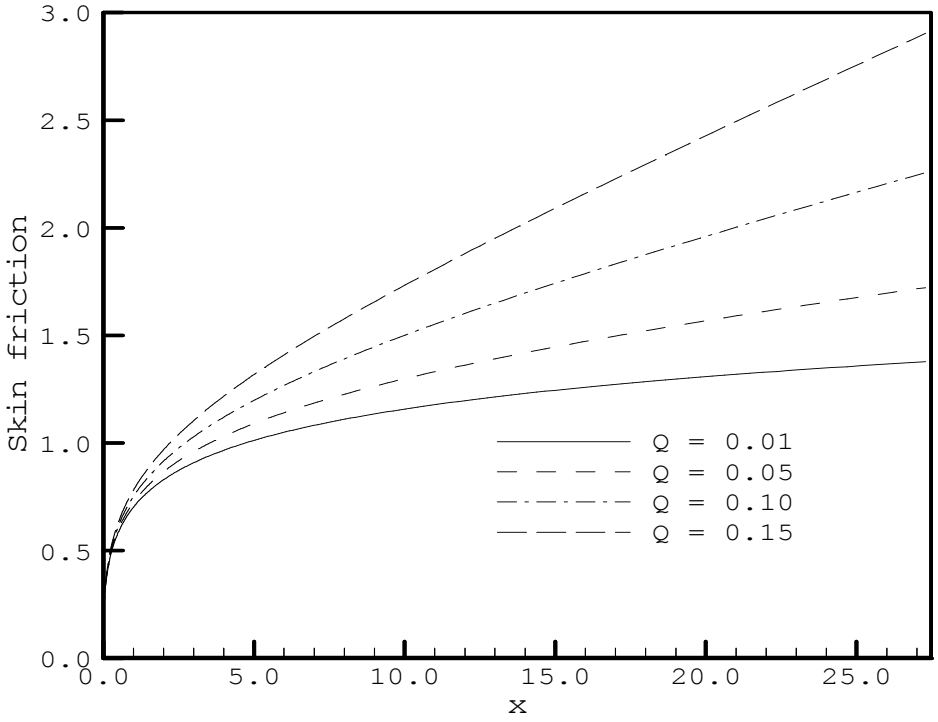

Figure 2.15: Variation of skin friction coefficient for different value of Q with $M = 0.10$, $Pr = 0.72$ and $\gamma = 0.10$

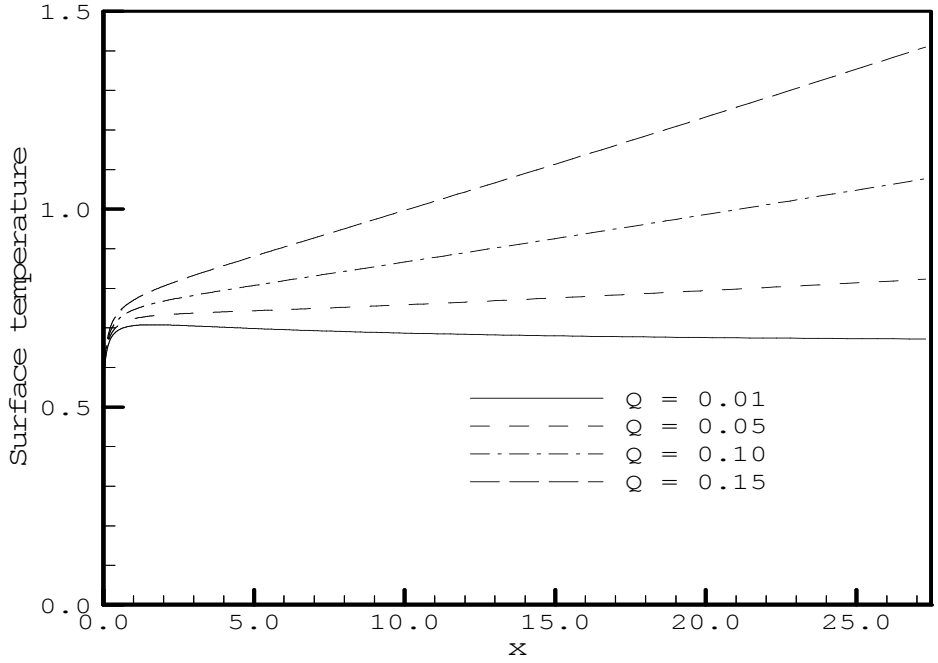

Figure 2.16: Variation of surface temperature profiles for different value of Q with $M = 0.10$, $Pr = 0.72$ and $\gamma = 0.10$

It is also observed that if the maximum values of the parameters (magnetic, thermal conductivity and heat generation) are increased then the data is coming down by using the program. As a result the graphs of velocity, temperature, skin friction coefficient and surface temperature profiles are not as well as before with respect to corresponding parameters.

2.5 Comparison of the results

Table 2.1 and 2.2 depict the comparisons of the present numerical results of the skin friction co-efficient C_{fx} and the surface temperature θ(x, 0) with those obtained by Pozzi and Lupo (1988) and Merkin and Pop (1996) respectively. Here, the magnetic parameter M, thermal conductivity variation parameter γ and heat generation parameter Q are ignored and the Prandtl number $Pr = 0.733$ with $x^{1/5} = \xi$ is chosen. It is clearly seen that there is an excellent agreement among the present results with the solutions of Pozzi and Lupo (1988) and Merkin and Pop (1996).

Table 2.1: Comparison of the present numerical results of skin friction coefficient with Prandtl number $Pr = 0.733$, $M = 0$, $\gamma = 0$ and $Q = 0$

C_{fx}			
$x^{\frac{1}{5}} = \xi$	Pozzi and Lupo (1988)	Merkin and Pop (1996)	Present work
0.7	0.430	0.430	0.419
0.8	0.530	0.530	0.517
0.9	0.635	0.635	0.613
1.0	0.741	0.745	0.712
1.1	0.829	0.859	0.801
1.2	0.817	0.972	0.890

Table 2.2: Comparison of the present numerical results of surface temperature profiles with Prandtl number $Pr = 0.733$, $M = 0$, $\gamma = 0$ and $Q = 0$

$\theta(x,0)$			
$x^{\frac{1}{5}} = \xi$	Pozzi and Lupo (1988)	Merkin and Pop (1996)	Present work
0.7	0.651	0.651	0.638
0.8	0.684	0.686	0.662
0.9	0.708	0.715	0.676
1.0	0.717	0.741	0.681
1.1	0.699	0.762	0.681
1.2	0.640	0.781	0.676

2.6 Summary and Conclusion of this chapter

The effects of the thermal conductivity variation due to temperature and conduction on Magnetohydrodynamic (MHD) free convection flow along a vertical flat plate with heat generation has been studied. From the present investigation the following conclusions may be drawn

- The velocity within the boundary layer increases for the decreasing value of M, Pr and the increasing value of γ, Q.
- The temperature increases for the increasing value of M, Q, γ and the decreasing value of Pr.
- The skin friction coefficient decreases for the increasing value of M and Pr and the decreasing values of γ, Q.
- An increased in the values of the thermal conductivity variation parameter γ, heat generation parameter Q and magnetic parameter M leads to an increased in the surface temperature.
- The surface temperature decreases for the increasing value of Pr.

Chapter 3

Effects of Temperature Dependent Thermal Conductivity on Magnetohydrodynamic Free Convection Flow along a Vertical Flat Plate together with Heat Generation and Pressure Work

3.1 Introduction

Conjugate effects of temperature dependent thermal conductivity on MHD free convection flow along a vertical flat plate with heat generation and pressure work have been described in this chapter. The governing boundary layer equations are transformed into a non dimensional form and the resulting non linear system of partial differential equations are reduce to local non similarity equations which are solved numerically by very efficient implicit finite difference method together with Keller box technique. Numerically results are presented by velocity, temperature, skin friction coefficient and surface temperature profiles for magnetic parameter M, Prandtl number Pr, thermal conductivity variation parameter γ, heat generation parameter Q and pressure work parameter ε. In the following section detailed derivations of the governing equations for the flow and the method of solutions along with the results and discussions are presented.

3.2 Governing equations of the flow

In the presence of heat generation and pressure work with temperature dependent thermal conductivity, free convection flow of an electrically conducting, viscous and incompressible fluid along a vertical flat plate of length l and thickness b has been considered in this chapter. It is assumed that the temperature at the outside surface is maintained at a constant temperature T_b, where $T_b > T_\infty$, the ambient temperature of the fluid. A uniform magnetic field of strength H_0 is imposed along the $\bar{y}$-axis (Figure-3).

The governing equations of such flow under the usual boundary layer and the Boussinesq approximations can be written as

$$\frac{\partial \bar{u}}{\partial \bar{x}} + \frac{\partial \bar{v}}{\partial \bar{y}} = 0 \qquad (3.1)$$

$$\bar{u}\frac{\partial \bar{u}}{\partial \bar{x}}+\bar{v}\frac{\partial \bar{u}}{\partial \bar{y}}=\nu\frac{\partial^2 \bar{u}}{\partial \bar{y}^2}+g\beta(T_f-T_\infty)-\frac{\sigma H_0^2\,\bar{u}}{\rho} \tag{3.2}$$

$$\bar{u}\frac{\partial T_f}{\partial \bar{x}}+\bar{v}\frac{\partial T_f}{\partial \bar{y}}=\frac{1}{\rho C_p}\frac{\partial}{\partial \bar{y}}(\kappa_f\frac{\partial T_f}{\partial \bar{y}})+\frac{Q_0}{\rho C_p}\left(T_f-T_\infty\right)+\frac{T_f\beta\bar{u}}{\rho c_p}\left(\frac{\partial p}{\partial \bar{x}}\right) \tag{3.3}$$

Here β is coefficient of volume expansion. Consider the temperature dependent thermal conductivity, which is proposed by Charraudeau (1975), as follows

$$\kappa_f=\kappa_\infty[1+\delta(T_f-T_\infty)] \tag{3.4}$$

where, κ_∞ is the thermal conductivity of the ambient fluid and δ is defined as follows

$$\delta=\frac{1}{\kappa_f}\left(\frac{\partial \kappa}{\partial T}\right)_f \tag{3.5}$$

The appropriate boundary conditions to be satisfied by the above equations are (Hossain 1992, Chang 2006, Merkin & Pop 1996)

$$\left.\begin{aligned}&\bar{u}=0, \qquad \bar{v}=0\\ &T_f=T(\bar{x},0), \quad \frac{\partial T_f}{\partial \bar{y}}=\frac{\kappa_s}{b\kappa_f}(T_f-T_b)\end{aligned}\right\} \quad on \quad \bar{y}=0,\ \bar{x}>0$$
$$\bar{u}\to 0,\ T_f\to T_\infty \ \ as \quad \bar{y}\to\infty, \quad \bar{x}>0 \tag{3.6}$$

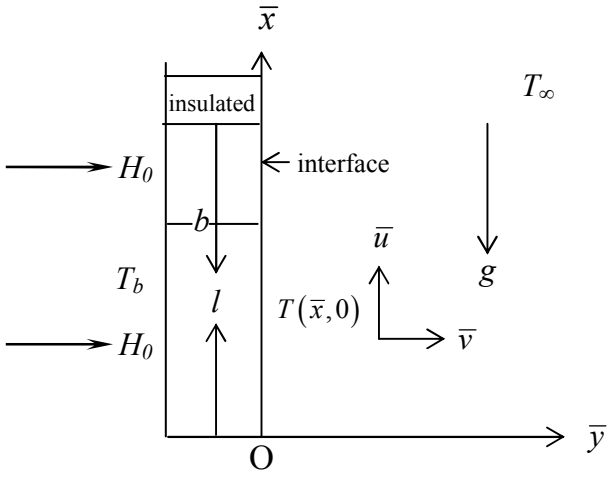

Figure 3: Physical model and coordinate system

Observed that the equations (3.2) and (3.3) together with the boundary conditions (3.6) are non-linear partial differential equations. In the following sections the solution methods of these equations are discussed in details.

3.3 Transformation of the governing equations

Equations (3.1) to (3.3) will be non-dimensionalized by using the following dimensionless variables

$$x=\frac{\bar{x}}{L},\ y=\frac{\bar{y}}{L}\,Gr^{\frac{1}{4}},\ u=\frac{\bar{u}L}{\nu}\,Gr^{-\frac{1}{2}},\ v=\frac{\bar{v}L}{\nu}\,Gr^{-\frac{1}{4}},\ \theta=\frac{T_f-T_\infty}{T_b-T_\infty},$$
$$Gr=\frac{g\,\beta L^3(T_b-T_\infty)}{\nu^2} \tag{3.7}$$

where, $L=\dfrac{\nu^{2/3}}{g^{1/3}}$ is reference length , Gr is the Grashof number, θ is the non dimensional temperature, $\nu=\mu/\rho$ is kinematic viscosity. As the problem of natural convection, its parabolic character has no characteristic length, L is the intrinsic properties of the system. It is along the y-direction has been modified by a factor $Gr^{1/4}$ in order to eliminate this quantity from the dimensionless equations and boundary conditions.

Substituting the relations (3.7) into the equations (3.1) to (3.3) then the following non-dimensional equations

$$\frac{\partial u}{\partial x}+\frac{\partial v}{\partial y}=0 \tag{3.8}$$

$$u\frac{\partial u}{\partial x}+v\frac{\partial u}{\partial y}+Mu=\frac{\partial^2 u}{\partial y^2}+\theta \tag{3.9}$$

$$u\frac{\partial \theta}{\partial x}+v\frac{\partial \theta}{\partial y}=\frac{1}{\mathrm{Pr}}(1+\gamma\theta)\frac{\partial^2\theta}{\partial y^2}+\frac{\gamma}{\mathrm{Pr}}\left(\frac{\partial\theta}{\partial y}\right)^2+Q\theta-\frac{g\beta\{T_\infty+(T_b-T_\infty)\theta\}}{C_P(T_b-T_\infty)} \tag{3.10}$$

where, $M=\dfrac{\sigma\,{H_0}^2L^2}{\mu\,Gr^{1/2}}$ is the dimensionless magnetic parameter, $\mathrm{Pr}=\dfrac{\mu\,C_p}{\kappa_\infty}$ is the Prandtl number, $\gamma=\delta(T_b-T_\infty)$ is the dimensionless thermal conductivity variation parameter, $Q=\dfrac{Q_0L^2}{\mu C_p Gr^{1/2}}$ is the dimensionless heat generation parameter and $\varepsilon=\dfrac{Gr\nu^2}{c_p\ L^2(T_b-T_\infty)}$ is the dimensionless pressure work parameter, $t_r=\dfrac{T_\infty}{(T_b-T_\infty)}$ is the temperature ratio parameter.

The corresponding boundary conditions (3.6) then take the following form

$$\begin{aligned} &u = 0, v = 0, \ \theta - 1 = (1+\gamma\theta)\ p\frac{\partial\theta}{\partial y} \quad on \ \ y = 0, x > 0 \\ &u \to 0, \theta \to 0 \quad as \ \ y \to \infty, x > 0 \end{aligned} \tag{3.11}$$

where, $p = \left(\frac{\kappa_\infty\, b}{\kappa_s L}\right) Gr^{\frac{1}{4}}$ is the conjugate conduction parameter. In actual fact, magnitude of O(p) depends on b/L and $Gr^{1/4}$ being the order of unity. L is small, the term b/L becomes greater than one. For air, $\frac{\kappa_\infty}{\kappa_s}$ attains very small values if the plate is highly conductive and reaches the order of 0.1 for materials such as glass. Therefore in different cases p is different but not always a small number. In the present investigation we have considered p = 1 which is accepted for b/L of O ($\frac{\kappa_\infty}{\kappa_s}$).

To solve the equations (3.9) and (3.10) subject to the boundary conditions (3.11) the following transformations are introduced (Merkin & Pop 1996)

$$\begin{aligned} \psi &= x^{\frac{4}{5}}(1+x)^{-\frac{1}{20}} f(x,\eta) \\ \eta &= y\, x^{-\frac{1}{5}}(1+x)^{-\frac{1}{20}} \\ \theta &= x^{\frac{1}{5}}(1+x)^{-\frac{1}{5}} h(x,\eta) \end{aligned} \tag{3.12}$$

here η is the similarity variable and ψ is the non-dimensional stream function which satisfies the continuity equation and is related to the velocity components in the usual way as $u = \frac{\partial\psi}{\partial y}$ and $v = -\frac{\partial\psi}{\partial x}$. Moreover, $h(x,\eta)$ represents the non-dimensional temperature. The momentum and energy equations (equations (3.9) and (3.10) respectively) are transformed for the new co-ordinate system. At first, the velocity components are expressed in terms of the new variables for this transformation.

Thus the following equations

$$\begin{aligned} f''' + \frac{16+15x}{20(1+x)} f f'' - \frac{6+5x}{10(1+x)} f'^2 - M\, x^{\frac{2}{5}}(1+x)^{\frac{1}{10}} f' \\ + h = x\left(f'\frac{\partial f'}{\partial x} - f''\frac{\partial f}{\partial x}\right) \end{aligned} \tag{3.13}$$

$$\frac{1}{\Pr}h'' + \frac{\gamma}{\Pr}\left(\frac{x}{1+x}\right)^{\frac{1}{5}}hh'' + \frac{\gamma}{\Pr}\left(\frac{x}{1+x}\right)^{\frac{1}{5}}h'^{2} + \frac{16+15x}{20(1+x)}fh' + Qx^{2/5}(1+x)^{1/10}h$$
$$-\varepsilon\left\{\left(\frac{1+x}{x}\right)^{1/5}\left(\frac{T_\infty}{T_b-T_\infty}\right)f' + hf'\right\} - \frac{1}{5(1+x)}fh = x\left(f'\frac{\partial h}{\partial x} - h'\frac{\partial f}{\partial x}\right) \tag{3.14}$$

where, prime denotes partial differentiation with respect to η. The boundary conditions as mentioned in equation (3.11) then take the following form

$$f(x,0) = f'(x,0) = 0$$
$$h'(x,0) = \frac{x^{\frac{1}{5}}(1+x)^{-\frac{1}{5}}h(x,0) - 1}{(1+x)^{-\frac{1}{4}} + \gamma\, x^{\frac{1}{5}}(1+x)^{-\frac{9}{20}}h(x,0)} \tag{3.15}$$
$$f'(x,\infty) \to 0, \quad h'(x,\infty) \to 0$$

The set of equations (3.13) and (3.14) together with the boundary conditions (3.15) are solved by applying implicit finite difference method with Keller (1978) box scheme. A good description of this method and its application to the boundary layer flow problems are given in the book by T. Cebeci and P. Bradshaw (1984). From the process of numerical computation, in practical point of view, it is important to calculate the values of the surface shear stress in terms of the skin friction coefficient. This can be written in the non-dimensional form as (Mamun et al. 2005)

$$C_f = \frac{Gr^{-\frac{3}{4}}L^2}{\mu\nu}\tau_w \tag{3.16}$$

where, $\tau_w[=\mu(\partial\bar{u}/\partial\bar{y})_{\bar{y}=0}]$ is the shearing stress. Using the new variables described in (3.7), the local skin friction co-efficient can be written as

$$C_{fx} = x^{\frac{2}{5}}(1+x)^{-\frac{3}{20}}f''(x,0) \tag{3.17}$$

The numerical values of the surface temperature distribution are obtained from the relation

$$\theta(x,0) = x^{\frac{1}{5}}(1+x)^{-\frac{1}{5}}h(x,0) \tag{3.18}$$

3.4 Results and Discussions

Solutions are obtained for the values of the Prandtl number Pr = 0.72, 0.93, 1.44, 1.63 and for a wide range of the magnetic parameter M = 0.10, 0.50, 0.90, 1.40, thermal conductivity γ = 0.05, 0.15, 0.30, 0.50, heat generation parameter Q =0.01, 0.05, 0.10, 0.15 and pressure work parameter ε = 0.01, 0.05, 0.09, 0.11, Detailed numerical results of the velocity, temperature, skin friction coefficient and surface temperature profiles for different values of magnetic parameter M, Prandtl number Pr, thermal conductivity variation parameter γ, heat generation parameter Q and pressure work parameter ε are presented graphically in figure 3.1 to 3.20.

Figures 3.1 and 3.2 display the velocity and temperature profiles for the different values of the magnetic parameter M. It is observed that as the magnetic parameter M increases, the velocity decreases between $0 \leq \eta \leq 4.59386$ and then increases with very small difference and finally approaches to zero along η direction. This is due to the fact that the velocity decreases rapidly for the small value of M comparatively, for the large value of M. The temperature increases with increasing value of the magnetic parameter M. This phenomenon can easily be understood from the fact that the interaction of the magnetic field and the moving electric charge carried by the flowing fluid induces a force, which tends to oppose the fluid motion and increases the temperature.

Figures 3.3 and 3.4 indicate the effects of the Prandtl number Pr on the velocity and temperature profiles. From figure 3.3, it is observed that the velocity decreases as well as its position moves toward the interface with the increasing value of Prandtl number Pr. The overall temperature also shift downwards with the increasing value of Pr as observed in figure 3.4. The physical fact is that the thermal boundary layer thickness decreases with increasing value of Pr that supports the result.

Figures 3.5 and 3.6 illustrate the velocity and temperature profiles for the different values of the thermal conductivity parameter γ. The velocity and the temperature increase within the boundary layer with the increasing value of γ. This is to be expected because the higher value of the thermal conductivity variation parameter accelerates the fluid flow and increases the temperature.

The effect of heat generation parameter Q on the velocity and the temperature within the boundary layer are shown in figures 3.7 and 3.8. It is seen from figures 3.7 and 3.8 that the velocity and temperature increase within the boundary layer with the increasing value

of the heat generation parameter Q. This phenomenon can easily be understood from the fact that the increased value of Q means that the more heat is produced and eventually that heat increases the fluid motion.

From figure 3.9, it is observed that an increased in the pressure work parameter ε, increases the velocity but near the surface of the plate and become maximum and then decreases and finally approaches to zero along η direction. The maximum values of the velocities are 0.49952, 0.51471, 0.52993, and 0.53755 for ε = 0.01, 0.05, 0.09, 0.11 respectively and each of which occurs at η = 1.42791. Here we found that the velocity increases by 7.61% as the value of ε increases from 0.01 to 0.11. Figure 3.10 shows the distribution of the temperature profiles for the value of the pressure work parameter ε = 0.01, 0.05, 0.09, 0.11. Clearly it is seen that the temperature increases owing to increasing values of the pressure work parameter ε and becomes maximum at the wall. The local maximum values of the temperature are 0.85854, 0.87777, 0.89786, 0.90823 for ε = 0.01, 0.05, 0.09, 0.11 respectively and each of which attains at the surface. Thus the temperature increases by 5.79% as the value of ε increases from 0.01 to 0.11.

It can easily be seen that the effect of the magnetic parameter M leads to a decreased in the local skin friction coefficient in figure 3.11. This phenomenon can easily be understood from the fact that the magnetic parameter M increases the Lorentz force, which opposes the flow, therefore decreases the velocity gradient and hence the local skin friction coefficient C_{fx} decreases. Again figure 3.12 shows that the surface temperature $\theta(x,0)$ increases due to the increased value of the magnetic parameter M. It can also be seen that the surface temperature increases along the upward direction of the plate for a particular value of M. The magnetic field acts against the flow and reduces the skin friction and produces the temperature at the interface.

Figures 3.13 and 3.14 deal with the effect of Prandtl number Pr on local skin friction coefficient and surface temperature distribution. It can be observed from figure 3.13 that the skin friction coefficient increases monotonically for a particular value of Pr. It can also be noted that the skin friction coefficient decreases for the increasing value of Pr. From figure 3.14, it can be seen that the surface temperature decreases owing to the increasing value of the Prandtl number Pr along the positive x-direction.

Figures 3.15 and 3.16 illustrate the effect of thermal conductivity variation parameter γ on local skin friction coefficient and surface temperature distribution. From figure 3.15,

it is seen that the skin friction coefficient increases monotonically along the upward direction of the plate for a particular value of γ. It is also seen that the skin friction factor increases for the increasing value of γ. From figure 3.16, it is seen that the surface temperature increases for the increasing value of γ. This is to be expected because the higher value of the thermal conductivity variation parameter accelerates the fluid flow and increases the temperature.

The variation of the local skin friction coefficient and surface temperature distribution for different values of the heat generation parameter Q are illustrated in figures 3.17 and 3.18. From the figures it can be seen that the increased value of the heat generation parameter Q leads to an increased in local skin friction coefficient and surface temperature. These are expected, since the heat generation mechanism creates a layer of hot fluid near the surface and finally the resultant temperature of the fluid exceeds the surface temperature.

In figures 3.19 and 3.20, the effects of the pressure work parameter ε on local skin friction coefficient and surface temperature distribution are observed. From the figure 3.19, it can be seen that an increased in the values of ε leads to an increased in the value of skin friction coefficient. Also in figure 3.20, it is seen that the surface temperature increases with the increasing value of pressure work parameter ε.

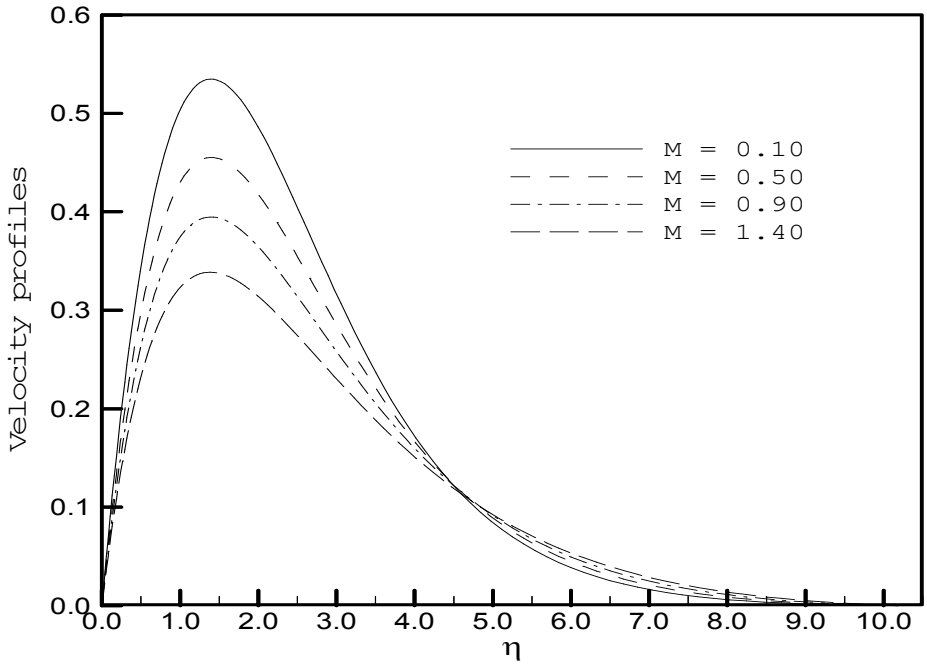

Figure 3.1: Variation of velocity profiles for different value of M with $Pr = 0.72$, $\gamma = 0.10$, $Q = 0.10$ and $\varepsilon = 0.10$

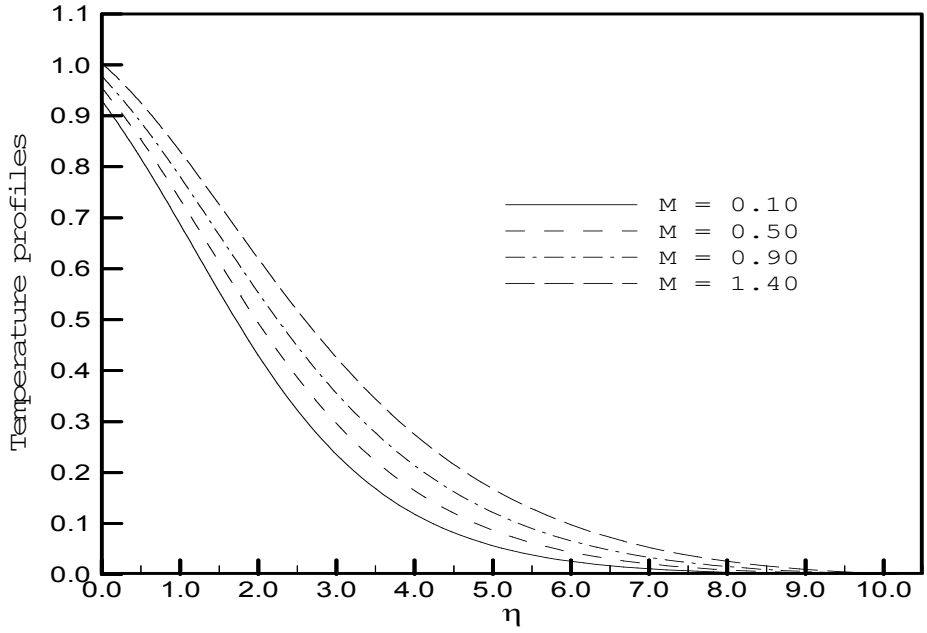

Figure 3.2: Variation of temperature profiles for different value of M with $Pr = 0.72$, $\gamma = 0.10$, $Q = 0.10$ and $\varepsilon = 0.10$

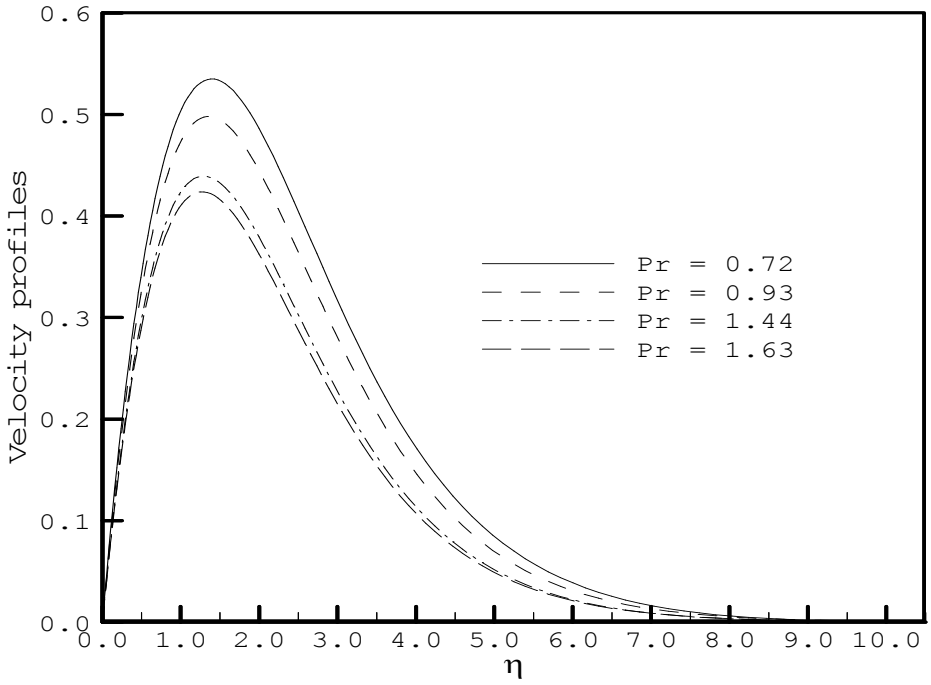

Figure 3.3: Variation of velocity profiles for different value of *Pr* with $M = 0.10$, $\gamma = 0.10$, $Q = 0.10$ and $\varepsilon = 0.10$

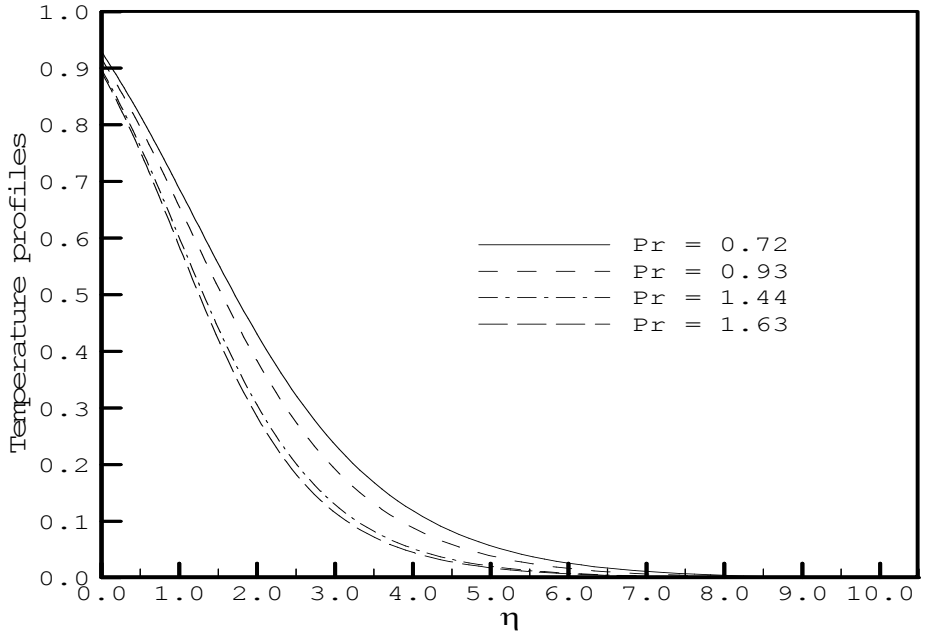

Figure 3.4: Variation of temperature profiles for different value of *Pr* with $M = 0.10$, $\gamma = 0.10$, $Q = 0.10$ and $\varepsilon = 0.10$

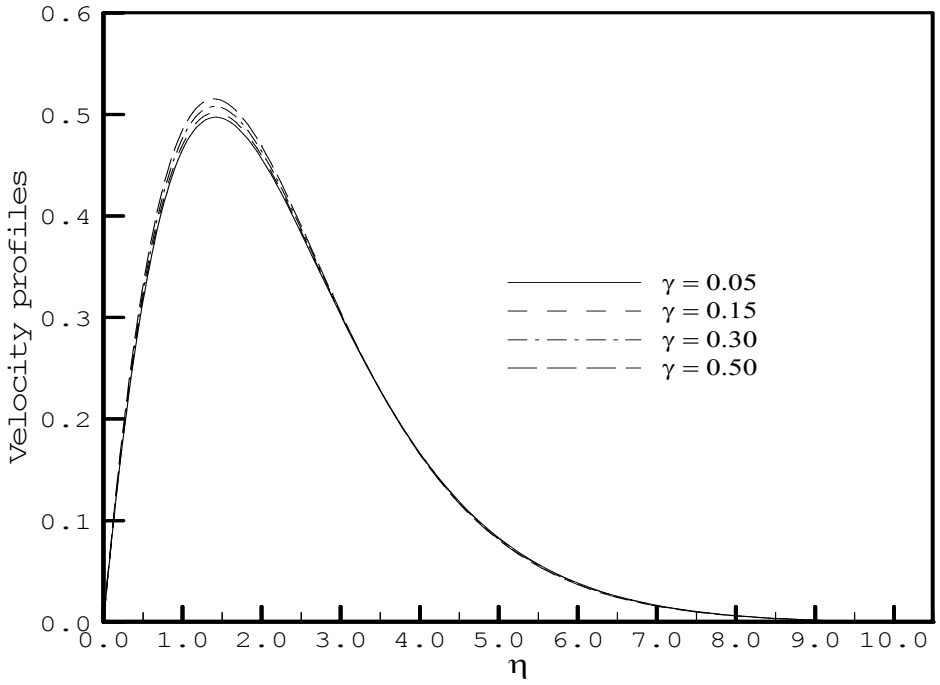

Figure 3.5: Variation of velocity profiles for different value of γ with $M = 0.10$, $Pr = 0.72$, $Q = 0.10$ and $\varepsilon = 0.01$

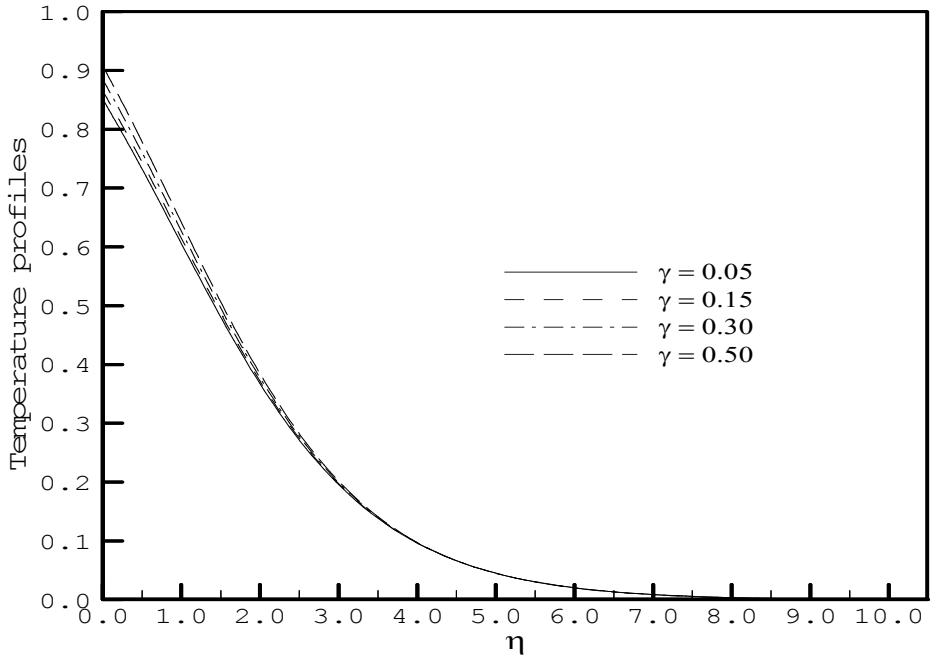

Figure 3.6: Variation of temperature profiles for different value of γ with $M = 0.10$, $Pr = 0.72$, $Q = 0.10$ and $\varepsilon = 0.01$

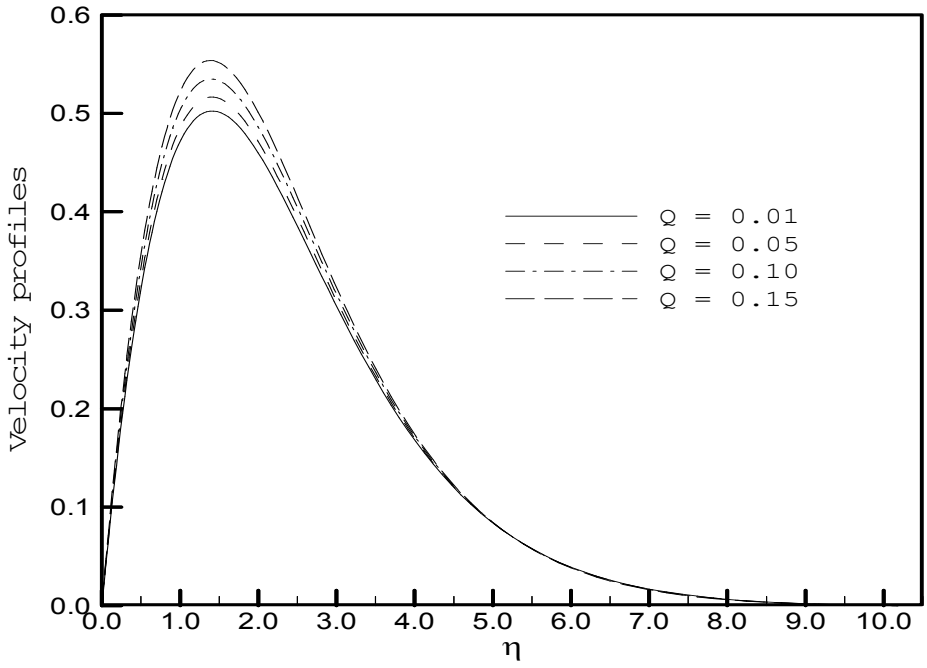

Figure 3.7: Variation of velocity profiles for different value of Q with $M = 0.10$, $Pr = 0.72$, $\gamma = 0.10$ and $\varepsilon = 0.10$

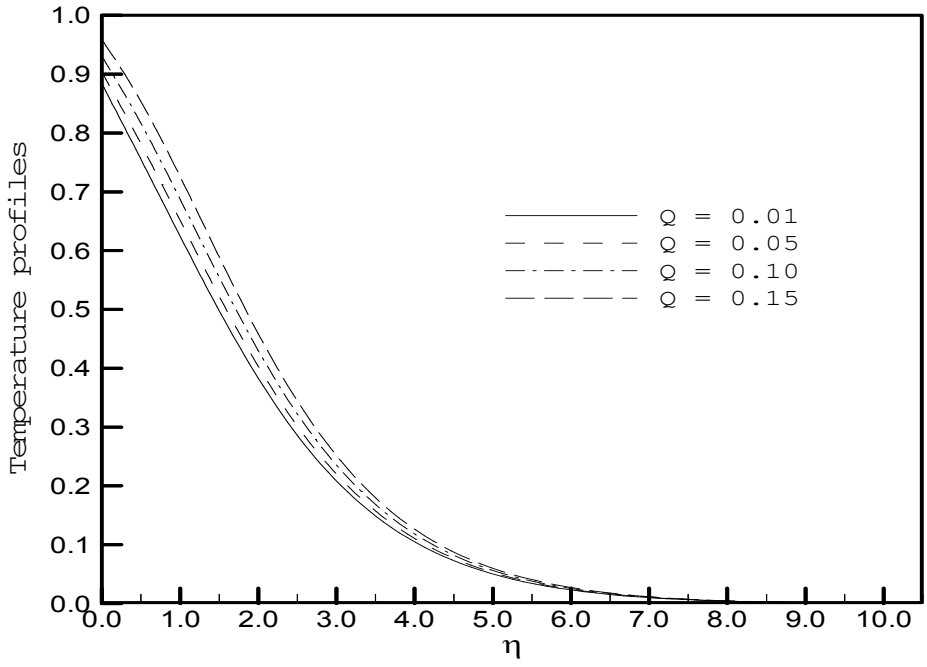

Figure 3.8: Variation of temperature profiles for different value of Q with M= 0.10, $Pr = 0.72$, $\gamma = 0.10$ and $\varepsilon = 0.10$

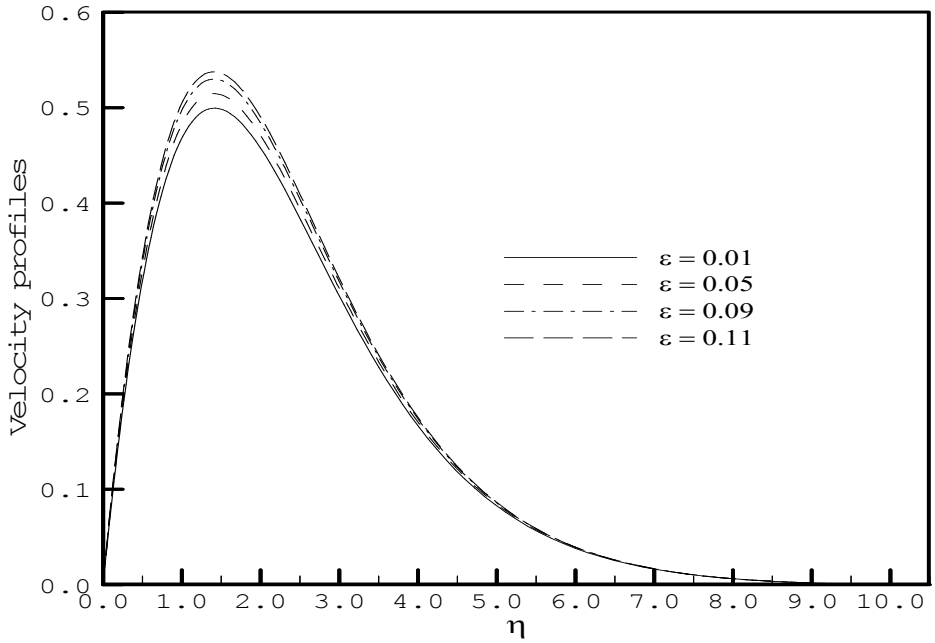

Figure 3.9: Variation of velocity profiles for different value of ε with $M = 0.10$, $Pr = 0.72$, $\gamma = 0.10$ and $Q = 0.10$

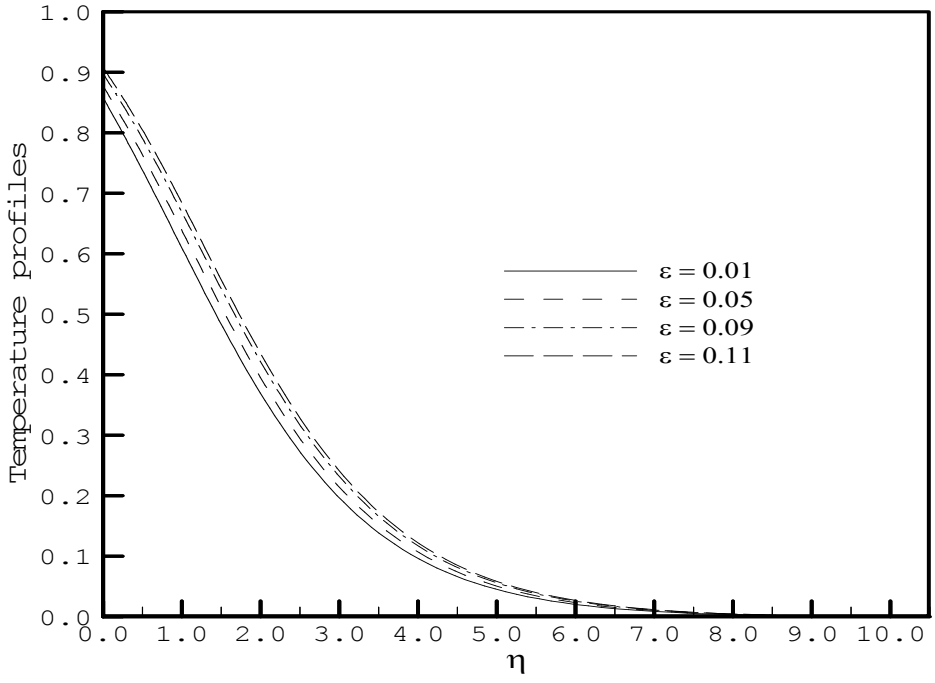

Figure 3.10: Variation of temperature profiles for different value of ε with M = 0.10, $Pr = 0.72$, $\gamma = 0.10$ and $Q = 0.10$

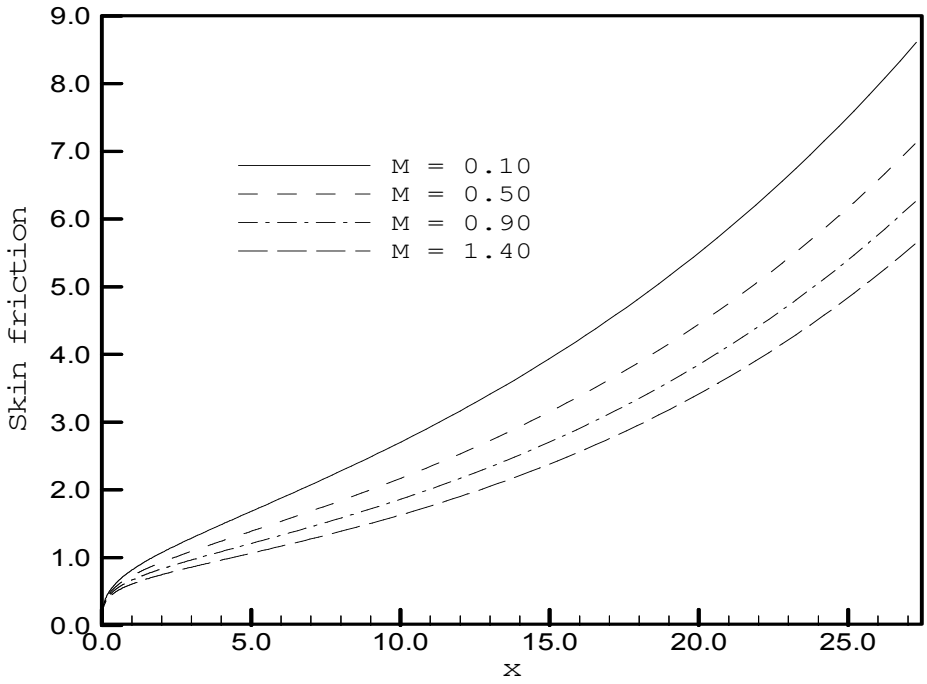

Figure 3.11: Variation of skin friction coefficient for different value of M with $Pr = 0.72$, $\gamma = 0.10$, $Q = 0.10$ and $\varepsilon = 0.10$

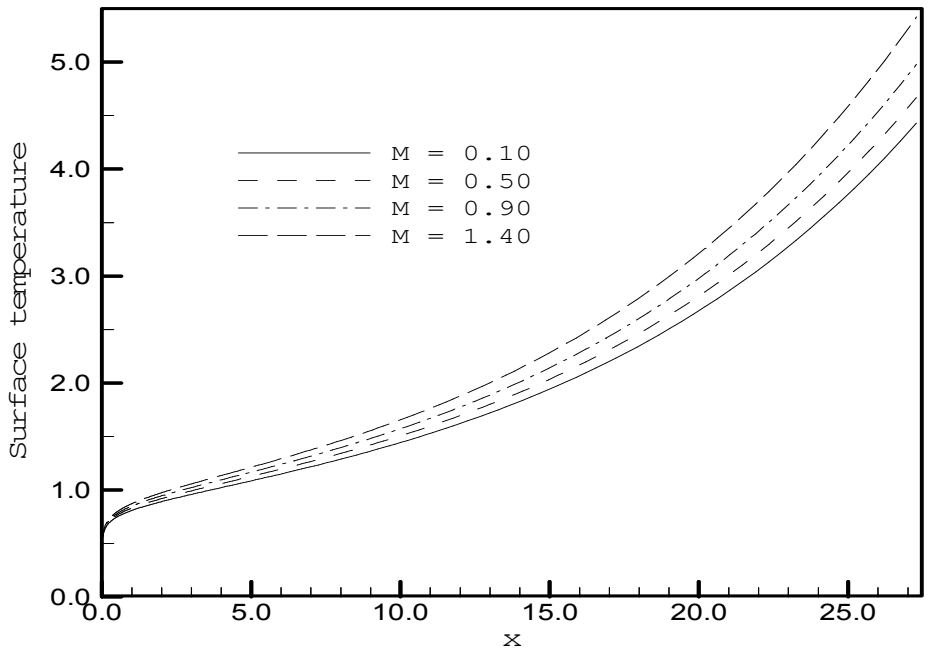

Figure 3.12: Variation of surface temperature profiles for different value of M with $Pr = 0.72$, $\gamma = 0.10$, $Q = 0.10$ and $\varepsilon = 0.10$

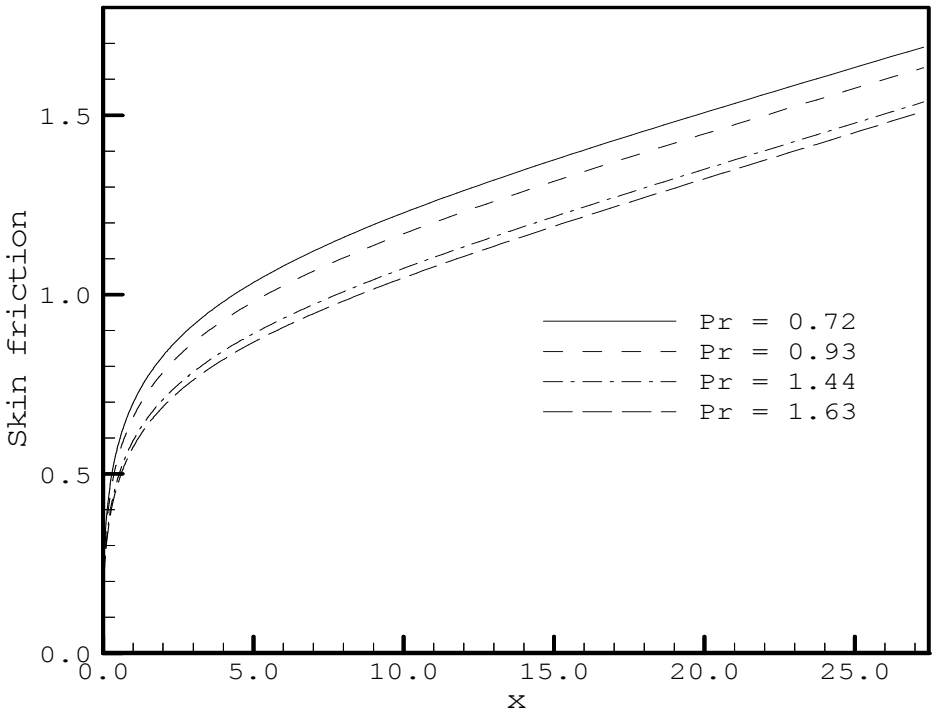

Figure 3.13: Variation of skin friction coefficient for different value of *Pr* with $M = 0.10$, $\gamma = 0.01$, $Q = 0.01$ and $\varepsilon = 0.01$

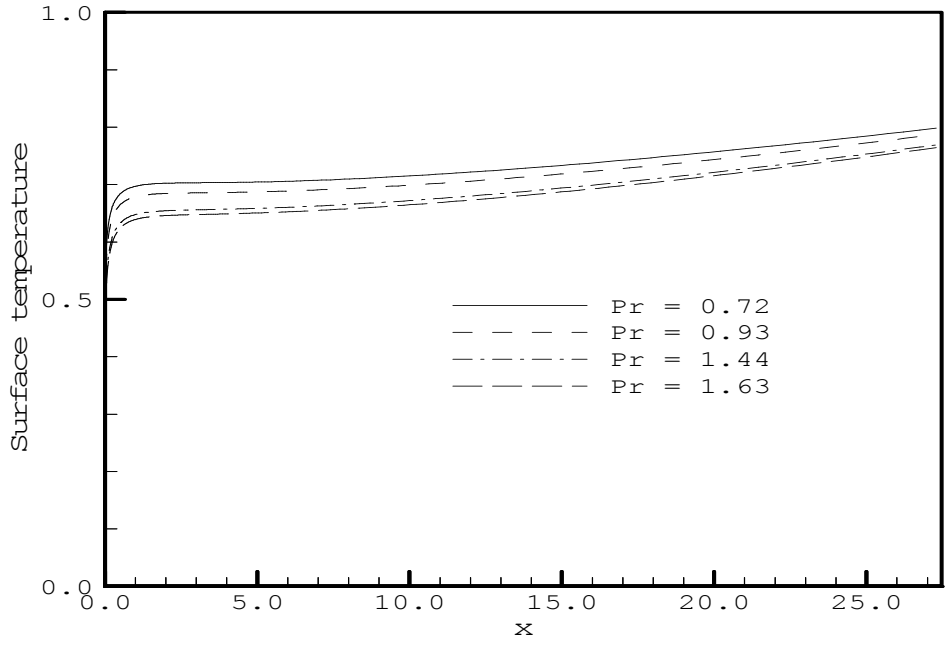

Figure 3.14: Variation of surface temperature profiles for different value of *Pr* with $M = 0.10$, $\gamma = 0.01$, $Q = 0.01$ and $\varepsilon = 0.01$

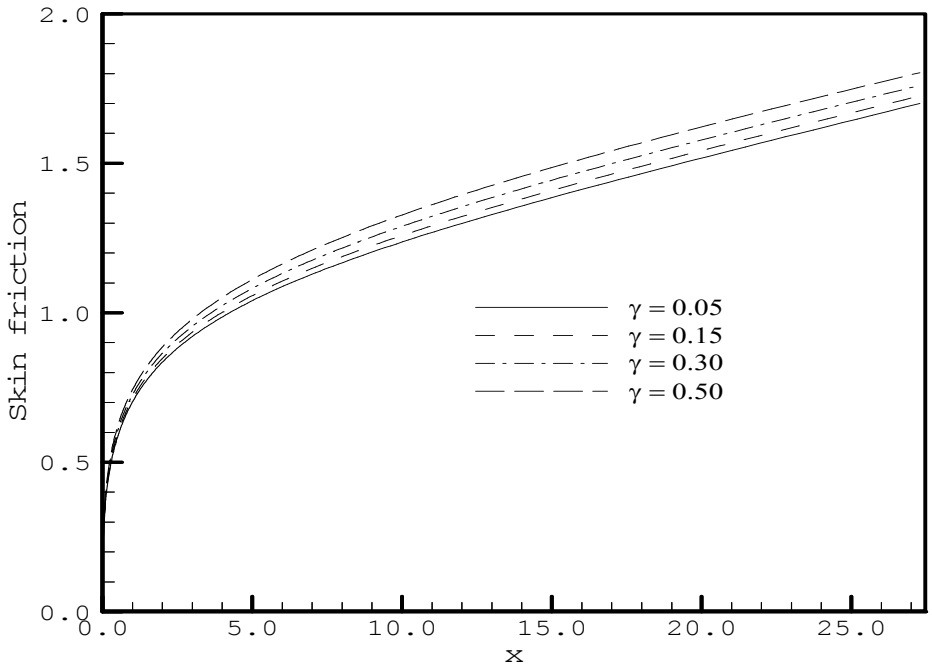

Figure 3.15: Variation of skin friction coefficient for different value of γ with $M = 0.10$, $Pr = 0.72$, $Q = 0.01$ and $\varepsilon = 0.01$

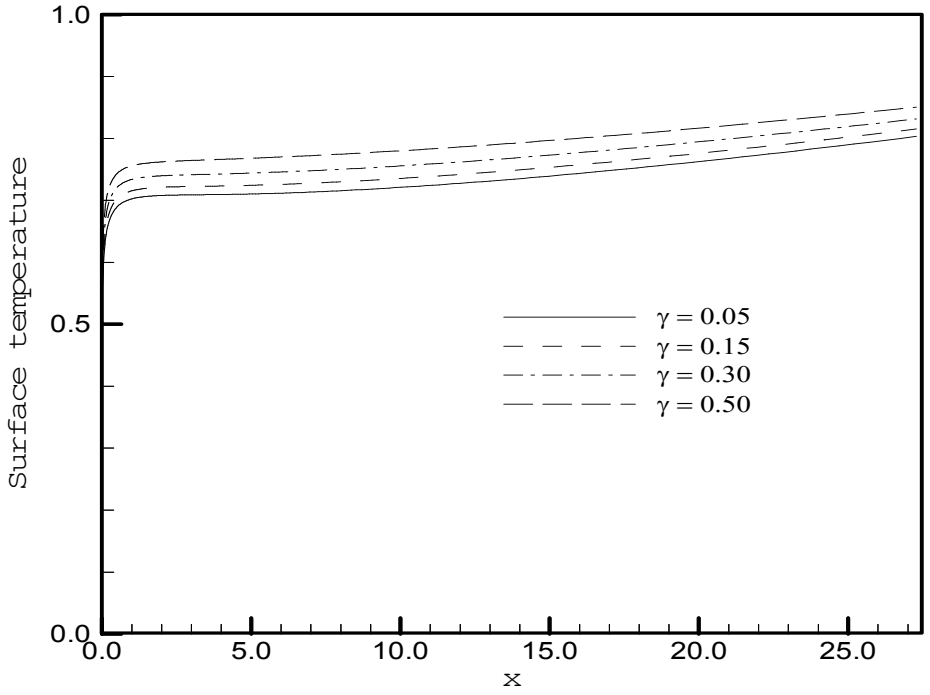

Figure 3.16: Variation of surface temperature profiles for different value of γ with $M = 0.10$, $Pr = 0.72$, $Q = 0.01$ and $\varepsilon = 0.01$

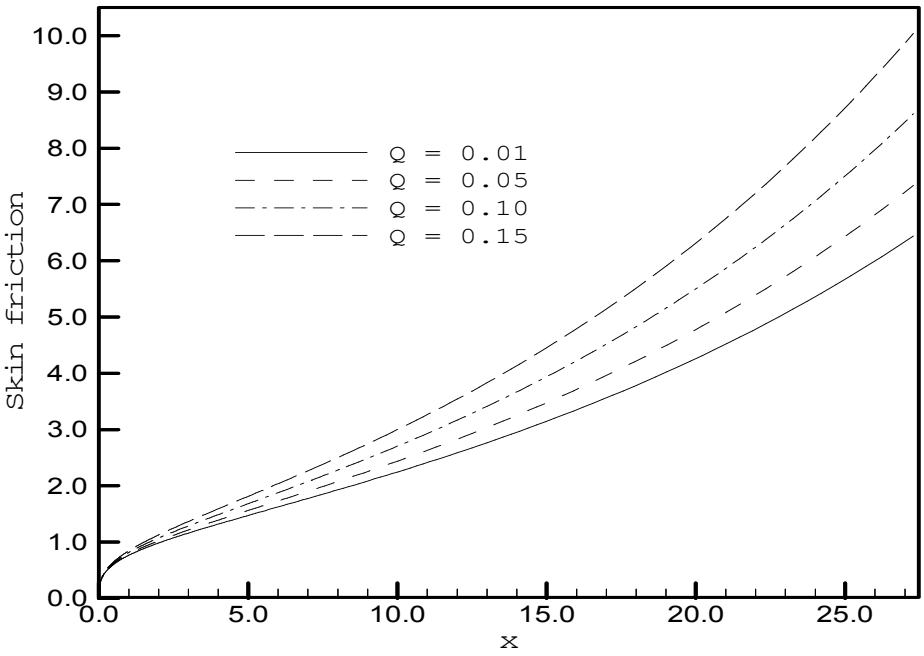

Figure 3.17: Variation of skin friction coefficient for different value of Q with $M = 0.10$, $Pr = 0.72$, $\gamma = 0.10$ and $\varepsilon = 0.10$

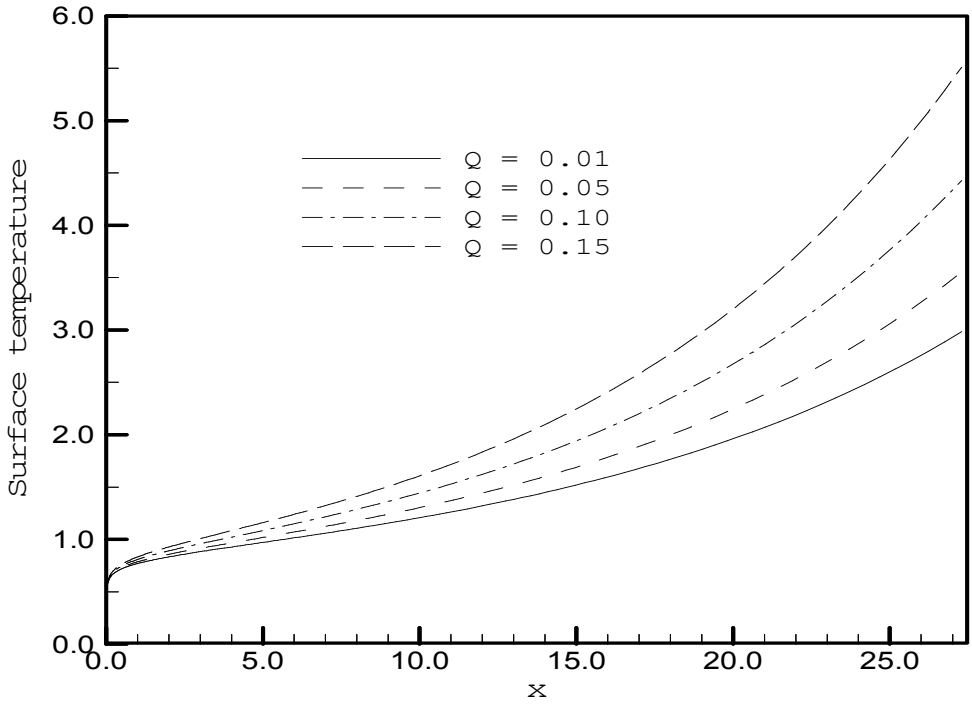

Figure 3.18: Variation of surface temperature profiles for different value of Q with $M = 0.10$, $Pr = 0.72$, $\gamma = 0.10$ and $\varepsilon = 0.10$

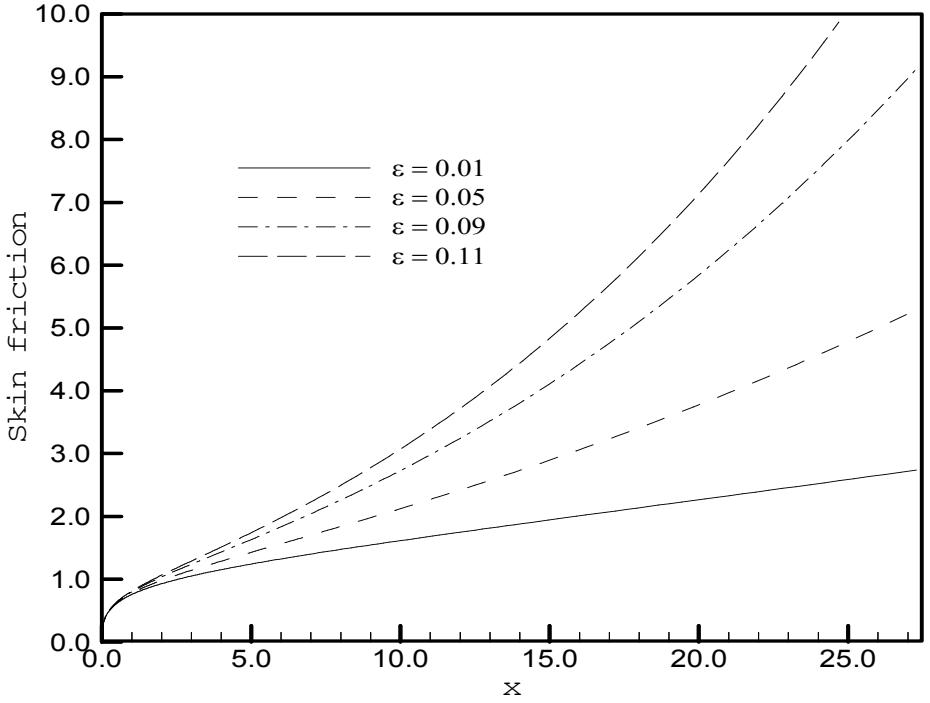

Figure 3.19: Variation of skin friction coefficient for different value of ε with $M = 0.10$, $Pr = 0.72$, $\gamma = 0.10$ and $Q = 0.10$

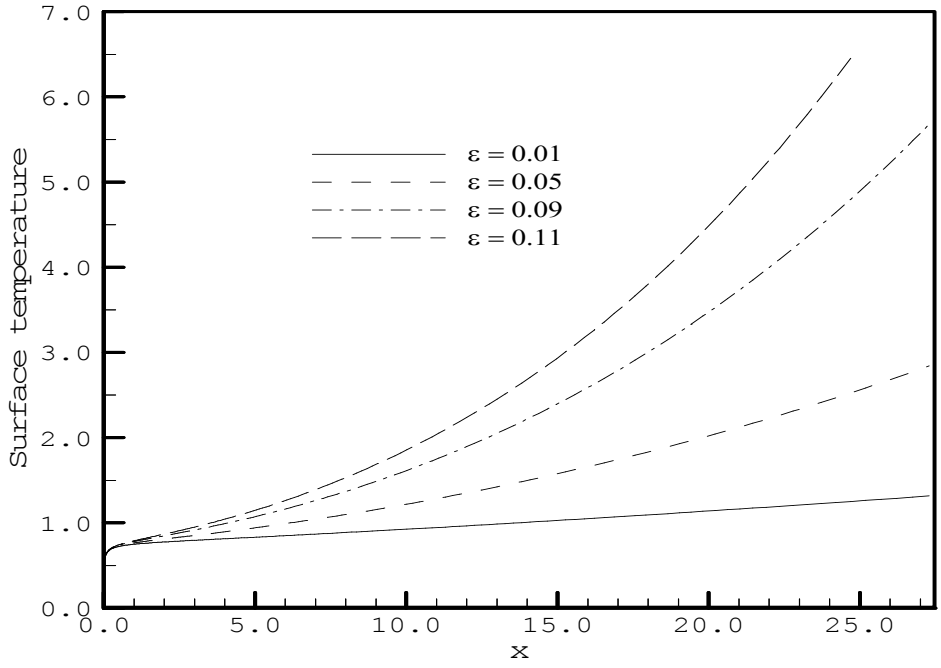

Figure 3.20: Variation of surface temperature profiles for different value of ε with $M = 0.10$, $Pr = 0.72$, $\gamma = 0.10$ and $Q = 0.10$

It is also observed that if the maximum values of the parameters (magnetic, thermal conductivity, heat generation and pressure work) are increased then the data is coming down by using the program. As a result the graphs of velocity, temperature, skin friction coefficient and surface temperature profiles are not as well as before with respect to corresponding parameters.

3.5 Comparison of the results

Table 3.1 and 3.2 depict the comparisons of the present numerical results of the skin friction co-efficient C_{fx} and the surface temperature θ(x, 0) with those obtained by Pozzi and Lupo (1988) and Merkin and Pop (1996) respectively. Here, the magnetic parameter M, thermal conductivity variation parameter γ, heat generation parameter Q and pressure work parameter ε are ignored and the Prandtl number Pr = 0.733 with $x^{1/5} = \xi$ is chosen. It is clearly seen that there is an excellent agreement among the present results with the solutions of Pozzi and Lupo (1988) and Merkin and Pop (1996).

Table 3.1: Comparison of the present numerical results of skin friction coefficient with Prandtl number Pr = 0.733, M = 0, γ = 0, Q = 0 and ε = 0

C_{fx}			
$x^{\frac{1}{5}} = \xi$	Pozzi and Lupo (1988)	Merkin and Pop (1996)	Present work
0.7	0.430	0.430	0.419
0.8	0.530	0.530	0.517
0.9	0.635	0.635	0.613
1.0	0.741	0.745	0.712
1.1	0.829	0.859	0.801
1.2	0.817	0.972	0.890

Table 3.2: Comparison of the present numerical results of surface temperature profiles with Prandtl number $Pr = 0.733$, $M = 0$, $\gamma = 0$, $Q = 0$ and $\varepsilon = 0$

$\theta(x,0)$			
$x^{\frac{1}{5}} = \xi$	Pozzi and Lupo (1988)	Merkin and Pop (1996)	Present work
0.7	0.651	0.651	0.638
0.8	0.684	0.686	0.662
0.9	0.708	0.715	0.676
1.0	0.717	0.741	0.681
1.1	0.699	0.762	0.681
1.2	0.640	0.781	0.676

3.6 Summary and Conclusion of this chapter

Conjugate effects of temperature dependent thermal conductivity on MHD free convection flow along a vertical flat plate with heat generation and pressure work has been studied. From the present investigation the following conclusions may be drawn

- The velocity within the boundary layer increases for the decreasing values of the magnetic parameter M, Prandtl number Pr and increasing values of the thermal conductivity variation parameter γ, heat generation parameter Q, and pressure work parameter ε.
- The temperature within the boundary layer increases for the increasing value of magnetic parameter M, thermal conductivity variation parameter γ, heat generation parameter Q and pressure work parameter ε and decreasing value of the Prandtl number Pr.
- The skin friction coefficient decreases for the increasing values of the magnetic parameter M, Prandtl number Pr and decreasing values of the thermal conductivity variation parameter γ, heat generation parameter Q and pressure work parameter ε.
- The surface temperature increases for the increasing values of the magnetic parameter M, thermal conductivity variation parameter γ, heat generation parameter Q, pressure work parameter ε and decreasing value of the Prandtl number Pr.

- The presence of a magnetic field normal to the flow in an electrically conducting fluid introduces a Lorentz force, which acts against the flow. This resistive force tends to slow down the flow and hence the fluid velocity decreases with the increase of the magnetic parameter. Since there is a friction between magnetic field and fluid flow produces heat, as a result the temperature profiles increase with the increase of the magnetic parameter and also surface temperature distribution increase with the increase of the magnetic parameter. Since the velocity decreases for the increasing value of magnetic parameter, so skin friction reduces for increasing value of magnetic parameter.
- Thermal conductivity depends on the temperature difference between the temperature outside the plate and the temperature outside the boundary layer. If this difference increases then also thermal conductivity increases, so increasing value of thermal conductivity variation parameter indicates the more heat transfer from plate to the boundary layer, which increases temperature distribution within the boundary layer and rapid mass transfer. Increasing velocity increases skin friction also surface temperature.
- The increase value of heat generation parameter Q and pressure work parameter ε means that more heat is produced and eventually, that heat increases the fluid motion. The heat generation and pressure work mechanism creates a layer of hot fluid near the surface and finally the resultant temperature of the fluid exceeds the surface temperature.

3.7 Extension of this work

The present work can be extended in different ways. Some of those are

- Temperature dependent thermal conductivity has been considered in the present study. For further extension temperature dependent viscosity of the fluid can be considered.
- The problem can be extended considering the Radiation heat transfer effects.
- Forced convection may be studied with the same geometry.
- It can also be considered for unsteady flow of the fluid.

References

Ahmad N. and Zaidi H. N., Magnetic effect on over back convection through vertical stratum, Proc. 2nd BSME-ASME International Conference on Thermal Engineering, pp. 157-168, 2004.

Alam, Md. M., Alim M. A. and Chowdhury Md. M. K., Effects of pressure stress work and viscous dissipation in the natural convection flow along a vertical flat plate with heat conduction, Journal of Naval Architecture and Marine Engineering 3, pp. 69-76, 2006.

Alam Md. M., Alim M. A. and Chowdhury M. K., Viscous dissipation effects on MHD natural convection flow over a sphere in the presence of heat generation, Nonlinear Analysis, Vol.12, No.4, pp. 447-459, 2007.

Al- Khawaja M. J., Agarwal R.K. and Gradner R.A., Numerical study of magneto fluid mechanics combined free and forced convection heat transfer, Int. J. Heat Mass Transfer, Vol.42, pp. 467-475, 1999.

Alim M.A, Alam M. and Abdullah Al-Mamun, Joule heating effect on the coupling of conduction with Magnetohydrodynamic free convection flow from a vertical flat plate.Nonlinear analysis, Vol.12, No.3, pp.307-316,2007.

Cebeci T. and Bradshaw P., Physical and Computational Aspects of Convective Heat Transfer, Springer, New York, 1984.

Charraudeau J., Influence de gradients de properties physiques en convection force application au cas du tube, Int. J. Heat Mass Transfer, Vol.18, pp.87-95, 1975.

Chen H. T and Chang S. M., The thermal interaction between laminar film condensation and forced convection along a conducting wall, Acta Mech., Vol.118, pp.13-26, 1996.

Chen L. C., A numerical simulation of micro polar fluid flows along a flat plate with wall conduction and buoyancy effects, J. Applied Physics. D, Vol.39, pp.1132- 1140, 2006.

Chen P., Combined free and forced convection flow about inclined surfaces in porous media, Int. J. Heat Mass Transfer, Vol.20, pp.807-814, 1977.

Chowdhury M. K. and Islam M. N., MHD free convection flow of visco-elastic fluid past an infinite porous plate, Heat Mass Transfer, Vol.36, pp. 439-447, 2000.

Clarke J.F. and Riley N., Natural convection induced in a gas by the presence of a hot porous horizontal surface, Q. J. Mech. Appl. Math., Vol.28, pp.373–396, 1975

Clarke J. F. and Riley N., Free convection and the burning of a horizontal fuel surface, J. Fluid Mech., Vol. 74, pp. 415–431, 1976.

Elbashbeshy E. M. A., Free convection flow with variable viscosity and thermal diffusivity along a vertical plate in the presence of magnetic field, International Journal Engineering Science, Vol.38, pp. 207-213, 2000.

Grander R.A. and Lo Y.T., Combined free and forced convection heat transfer in magneto fluid mechanic pipe flow, AICHE, Vol. 73, No. 164, p.133, 1975.

Hassanien I.A., Combined forced and free convection in boundary layer flow of a micro polar fluid over a horizontal plate, ZAMP, Vol. 48, No.4, p. 571, 1977.

Hossain M .A., Das S. K. and Pop, I., Heat transfer response of MHD free convection flow along a vertical plate to surface temperature oscillation, Int. J. Non-Linear Mechanics, Vol. 33, No.3, pp.541-553, 1998.

Hossain M.A. and Ahmad M., MHD forced and free convection boundary layer flow near the leading edge, Int. J. Heat Mass Transfer, Vol.33 ,No.3, pp.571-575, 1990.

Hossain M. A, The viscous and Joule heating effects on MHD free convection flow with variable plate temperature, Int. J. Heat Mass Transfer, Vol. 35, No. 12, pp.3485-3487, 1992.

Hossain M.A., Alam K.C.A. and Rees D.A.S., MHD forced and free convection boundary layer flow along a vertical porous plate, Applied Mechanics and Engineering, Vol.2, No.1, pp.33-51, 1997.

Keller H. B., Numerical methods in boundary layer theory, Annual Rev. Fluid Mechanics, Vol. 10, pp. 417-433, 1978.

Khan Z. I., Conjugate effect of conduction and convection with natural convection flow from a vertical flat plate and in an inclined square cavity, M. Phil thesis, Department of Mathematics, BUET, (2002).

Lin H.T. and Yu W.S., Free convection on a horizontal plate with blowing and suction, J. Heat Trans., ASME, Vol.110, pp.793–796, 1988.

Luikov A. K., Conjugate convective heat transfer problems, Int. J. Heat Mass Transfer, Vol.16, pp. 257-265, 1974.

Mamun M. M., Azad R. and Lineeya T. R., Natural convection flow from an isothermal sphere with temperature dependent thermal conductivity, Journal of Architecture and Marine Engineering, Vol.2, pp.53-64, 2005.

Mamun, A. A., Azim, N. H. Md. and Maleque, Md. A., Combined Effect of Conduction and Viscous Dissipation on MHD Free Convection Flow along a Vertical Flat Plate, Journal of Naval Archit. and Marine Eng., Vol.4, pp.87-98, 2007..

Mamun, A. A., Chowdhury, Z. R., Azim M. A. and Maleque M. A., Conjugate heat transfer for a vertical flat plate with heat generation effect, Nonlinear Analysis: Modeling and Control, Vol.13, No.2, pp. 213-223, 2008.

Mamun, A. A., Chowdhury, Z. R., Azim M. A. and Molla M. M., MHD- Conjugate heat transfer analysis for a vertical flat plate in the presence of viscous dissipation and heat

generation, International Communications in heat and mass transfer, 35, pp. 1275-1280, 2008.

Mendez F., Trevino C., The conjugate conduction-natural convection heat transfer along a thin vertical plate with non-uniform internal heat generation, Int. J. Heat and Mass Transfer, Vol. 43, pp. 2739-2748, 2000.

Merkin J. H and Pop I., Conjugate free convection on a vertical surface, Int. J. Heat Mass Transfer, Vol. 39, pp.1527- 1534, 1996.

Merkin J.H. and Mahmood T., On the free convection boundary layer on a vertical plate with prescribed surface heat flux, J. Engg. Math, Vol. 24, pp. 95-107, 1990.

Miyamoto M., Sumikawa J., Akiyoshi T. and Nakamura T., The effect of axial heat conduction in a vertical flat plate on free convection heat transfer, Int. J. Heat Mass Transfer, Vol.23, No.11, pp.1545-1553, 1980.

Pop I., Lesnic D. and Ingham D. B., The conjugate mixed convection on a vertical surface in porous medium, Int. J. Heat Mass Transfer, Vol. 38, No.8 pp.1517-1525, 1995.

Pop I., Ingham D.B., Convective heat transfer, Pergamon, Oxford 179, 2001.

Pozzi A. and Lupo M., The coupling of conduction with laminar convection along a flat plate, Int. J. Heat Mass Transfer, Vol.31, No. 9,pp.1807-1814, 1988.

Raisinghania M. D., Fluid Dynamics, S. Chand & Company Ltd., New Delhi, 2003.

Rahman M. M., Mamun A. A., Azim M. A., Alim M. A., Effects of temperature dependent thermal conductivity on magnetohydrodynamic free convection flow along a vertical flat plate with heat conduction, Nonlinear Analysis: Modelling and Control, Vol. 13, No. 4, pp. 513-524, 2008.

Raptis A. and Kafoussias N., Magnetohydrodynamic free convection flow and mass transfer through a porous medium bounded by an infinite vertical porous plate with constant heat flux, Canadian Journal of Physics, Vol. 60 No. 12, pp.1725-1729, 1982.

Shu J. J. and Pop I., The thermal interaction between free convection and forced convection along a vertical conducting wall, Int. J. Heat Mass Transfer, Vol.35, pp.33-38, 1999.

Takhar H. S. and Soundalgekar V. M., Dissipation effects on MHD free convection flow past a semi-infinite vertical plate, Applied Scientific Research, Vol. 36, No. 3, pp. 163-171, 1980.

Vedhanayagam M., Altenkirch R. A. and Eichhorn R., A transformation of the boundary layer equations for free convection past a vertical flat plate with arbitrary blowing and wall temperature variations, Int. J. Heat Mass Transfer, Vol.23 , pp.1286-1288, 1980.

.

Appendix

Implicit Finite Difference Method

To get the solutions of the transformed governing equations (2.13) and (2.14) along with the boundary condition (2.15), we employed implicit finite difference method together with Keller box elimination technique, which is well documented and widely used by H. B. Keller (1978) and T. Cebeci and P. Bradshow(1984).

To apply the aforementioned method, we first convert equations (2.13) and (2.14) into the following system of first order equations with dependent variables $u(\xi,\eta),\ v(\xi,\eta),\ p(\xi,\eta)$ and g (ξ,η) as

$$f' = u,\ u' = v,\ g' = p \tag{A1}$$

$$v' + p_1 f\, v - p_2 u^2 - p_4 u + g = \xi(u\frac{\partial u}{\partial \xi} - v\frac{\partial f}{\partial \xi}) \tag{A2}$$

$$\frac{1}{\Pr} p' + p_1 f\, p - p_3 u\, g + \frac{p_5}{\Pr} g\, p' + \frac{p_5}{\Pr} p^2 + p_6 g = \xi\ (u\ \frac{\partial g}{\partial \xi} - p\ \frac{\partial f}{\partial \xi}) \tag{A3}$$

where, ξ = x, h = g and

$$p_1 = \frac{16+15x}{20(1+x)},\ p_2 = \frac{6+5x}{10(1+x)},\ p_3 = \frac{1}{5(1+x)},\ \ p_4 = M\, x^{\frac{2}{5}} (1+x)^{\frac{1}{10}}, p_5 = \left(\frac{x}{1+x}\right)^{\frac{1}{5}} \gamma,$$

$$P_6 = Q\, x^{\frac{2}{5}} (1+x)^{1/10}$$

And the boundary conditions are

$$f(\xi,0) = 0,\ u(\xi,0) = 0$$

$$p(\xi,0) = \frac{\xi^{\frac{1}{5}} (1+\xi)^{-\frac{1}{5}} g\ (\xi,0) - 1}{(1+\xi)^{-\frac{1}{4}} + \gamma\, \xi^{\frac{1}{5}} (1+\xi)^{-\frac{9}{20}} g(\xi,0)} \tag{A4}$$

$$u(\xi,0) = 0,\ g\ (\xi,0) = 0$$

Now consider the net rectangle on the (ξ,η) plane shown in the figure A-1 and denote the net points by

$$\xi^0 = 0,\ \xi^n = \xi^{n-1} + k_n,\ n = 1, 2, 3, \cdots, N$$
$$\eta_0 = 0,\ \eta_j = \eta_{j-1} + h_{j,}\quad j = 1, 2, 3, \cdots, J$$

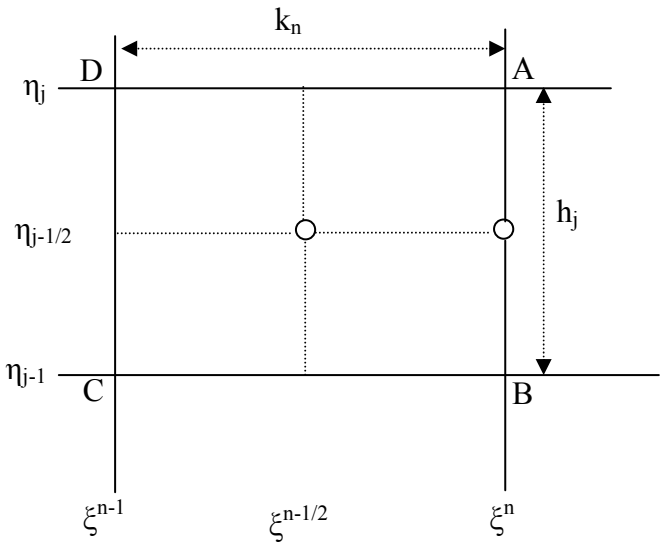

Figure A-1: Net rectangle for difference approximations for the Box scheme.

here, n and j are just sequence of numbers on the *(ξ,η)* plane, k_n and h_j are the variable mesh widths. Approximate the quantities f, u, v, p at the points *(ξ^n, η_j)* of the net by $f_j^n,\ u_j^n, v_j^n,\ p_j^n$ which call net function. We also employ the notation P_j^n for the quantities midway between net points shown in figure A-1 and for any net function as

$$\xi^{n-1/2} = \frac{1}{2}(\xi^n + \xi^{n-1}) \tag{A5}$$

$$\eta_{j-1/2} = \frac{1}{2}(\eta_j + \eta_{j-1}) \tag{A6}$$

$$g_j^{\,n-1/2} = \frac{1}{2}(g_j^{\,n} + g_j^{\,n-1}) \tag{A7}$$

$$g_{j-1/2}^n = \frac{1}{2}(g_j^n + g_{j-1}^n) \tag{A8}$$

The finite difference approximations according to box method to the three first order ordinary differential equations (A1) are written for the mid point *$(\xi^n, \eta_{j-1/2})$* of the segment *AB* shown in the figure A-1 and the finite difference approximations to the two

first order differential equations (A2) and (A3) are written for the mid point $(\xi^{n-1/2}, \eta_{j-1/2})$ of the rectangle $ABCD$. This procedure yields

$$\frac{f_j^n - f_{j-1}^n}{h_j} = u_{j-1/2}^n = \frac{u_{j-1}^n + u_j^n}{2} \tag{A9}$$

$$\frac{u_j^n - u_{j-1}^n}{h_j} = v_{j-1/2}^n = \frac{v_{j-1}^n + v_j^n}{2} \tag{A10}$$

$$\frac{g_j^n - g_{j-1}^n}{h_j} = p_{j-1/2}^n = \frac{p_{j-1}^n + p_j^n}{2} \tag{A11}$$

$$\begin{aligned}&\frac{1}{2}\left(\frac{v_j^n - v_{j-1}^n}{h_j} + \frac{v_j^{n-1} - v_{j-1}^{n-1}}{h_j}\right) + p_1 (fv)_{j-1/2}^{n-1/2} - p_2 \left(u^2\right)_{j-1/2}^{n-1/2} - p_4 (u)_{j-1/2}^{n-1/2} \\ &+ g_{j-1/2}^{n-1/2} = \xi_{j-1/2}^{n-1/2} \left(u_{j-1/2}^{n-1/2} \frac{u_{j-1/2}^n - u_{j-1/2}^{n-1}}{k_n} - v_{j-1/2}^{n-1/2} \frac{f_{j-1/2}^n - f_{j-1/2}^{n-1}}{k_n}\right)\end{aligned} \tag{A12}$$

$$\begin{aligned}&\frac{1}{2P_r}\left(\frac{p_j^n - p_{j-1}^n}{h_j} + \frac{p_j^{n-1} - p_{j-1}^{n-1}}{h_j}\right) + p_1 (fp)_{j-1/2}^{n-1/2} - p_3 (ug)_{j-1/2}^{n-1/2} + \\ &+ \frac{p_5}{2\,\mathrm{Pr}} g_{j-1/2}^{n-1/2} \left(\frac{p_j^n - p_{j-1}^n}{h_j} + \frac{p_j^{n-1} - p_{j-1}^{n-1}}{h_j}\right) + \frac{p_5}{\mathrm{Pr}} \left(P^2\right)_{j-1/2}^{n-1/2} + p_6 g_{j-1/2}^{n-1/2} \\ &= \xi_{j-1/2}^{n-1/2} \left(u_{j-1/2}^{n-1/2} \frac{g_{j-1/2}^n - g_{j-1/2}^{n-1}}{k_n} - p_{j-1/2}^{n-1/2} \frac{f_{j-1/2}^n - f_{j-1/2}^{n-1}}{k_n}\right)\end{aligned} \tag{A13}$$

Now from the equation (A12) we have

$$\begin{aligned}&\Rightarrow \frac{1}{2}\left(\frac{v_j^n - v_{j-1}^n}{h_j}\right) + \frac{1}{2}\left(\frac{v_j^{n-1} - v_{j-1}^{n-1}}{h_j}\right) + \frac{1}{2} p_1 \left\{(fv)_{j-1/2}^n + (fv)_{j-1/2}^{n-1}\right\} \\ &- \frac{1}{2} p_2 \left\{(u^2)_{j-1/2}^n + (u^2)_{j-1/2}^{n-1}\right\} - \frac{1}{2} p_4 \left\{u_{j-1/2}^n + u_{j-1/2}^{n-1}\right\} \\ &+ \frac{1}{2}\left\{g_{j-1/2}^n + g_{j-1/2}^{n-1}\right\} = \frac{1}{2k_n} \xi_{j-1/2}^{n-1/2} \left(u_{j-1/2}^n + u_{j-1/2}^{n-1}\right)\left(u_{j-1/2}^n - u_{j-1/2}^{n-1}\right) \\ &- \frac{1}{2k_n} \xi_{j-1/2}^{n-1/2} \left(v_{j-1/2}^n + v_{j-1/2}^{n-1}\right)\left(f_{j-1/2}^n - f_{j-1/2}^{n-1}\right)\end{aligned}$$

$$\begin{aligned}&\Rightarrow h_j^{-1} \left(v_j^n - v_{j-1}^n\right) + p_1 (fv)_{j-1/2}^n - p_2 (u^2)_{j-1/2}^n - p_4 (u)_{j-1/2}^n + g_{j-1/2}^n \\ &= \alpha_n \left[\left\{(u^2)_{j-1/2}^n - (u)_{j-1/2}^n (u)_{j-1/2}^{n-1} + (u)_{j-1/2}^n (u)_{j-1/2}^{n-1}\right\}\right. \\ &\left. - \left\{v_{j-1/2}^n f_{j-1/2}^n - v_{j-1/2}^n f_{j-1/2}^{n-1} + f_{j-1/2}^n v_{j-1/2}^{n-1}\right\}\right] - \left[h_j^{-1} \left(v_j^{n-1} - v_{j-1}^{n-1}\right) + p_1 (fv)_{j-1/2}^{n-1} - \right. \\ &\left. p_2 (u^2)_{j-1/2}^{n-1} - p_4 (u)_{j-1/2}^{n-1} + g_{j-1/2}^{n-1}\right] + \alpha_n \left[-(u^2)_{j-1/2}^{n-1} + (fv)_{j-1/2}^{n-1}\right]\end{aligned}$$

$$\Rightarrow h_j^{-1}(v_j^n - v_{j-1}^n) + p_1 (fv)_{j-1/2}^n - p_2 (u^2)_{j-1/2}^n - p_4 (u)_{j-1/2}^n + g_{j-1/2}^n$$
$$- \alpha_n [\{(u^2)_{j-1/2}^n - (fv)_{j-1/2}^n + v_{j-1/2}^n f_{j-1/2}^{n-1} - f_{j-1/2}^n v_{j-1/2}^{n-1}\}]$$
$$= \alpha_n [(fv)_{j-1/2}^{n-1} - (u^2)_{j-1/2}^{n-1}] - L_{j-1/2}^{n-1}$$

$$where\ L_{j-1/2}^{n-1} = h_j^{-1}(v_j^{n-1} - v_{j-1}^{n-1}) + p_1 (fv)_{j-1/2}^{n-1} - p_2 (u^2)_{j-1/2}^{n-1} - p_4 (u)_{j-1/2}^{n-1} + g_{j-1/2}^{n-1}$$

$$\Rightarrow h_j^{-1}(v_j^n - v_{j-1}^n) + \{p_1 + \alpha_n\}(fv)_{j-1/2}^n - \{p_2 + \alpha_n\}(u^2)_{j-1/2}^n$$
$$- p_4 (u)_{j-1/2}^n + g_{j-1/2}^n + \alpha_n (f_{j-1/2}^n v_{j-1/2}^{n-1} - v_{j-1/2}^n f_{j-1/2}^{n-1})$$
$$= \alpha_n \{(fv)_{j-1/2}^{n-1} - (u^2)_{j-1/2}^{n-1}\} - L_{j-1/2}^{n-1}$$

$$\Rightarrow h_j^{-1}(v_j^n - v_{j-1}^n) + \{p_1 + \alpha_n\}(fv)_{j-1/2}^n - \{p_2 + \alpha_n\}(u^2)_{j-1/2}^n$$
$$- p_4 (u)_{j-1/2}^n + g_{j-1/2}^n + \alpha_n (f_{j-1/2}^n v_{j-1/2}^{n-1} - v_{j-1/2}^n f_{j-1/2}^{n-1}) \qquad \text{(A14)}$$
$$= R_{j-1/2}^{n-1}$$

where, $\alpha_n = \frac{1}{k_n}\xi_{j-1/2}^{n-1/2}$ and $R_{j-1/2}^{n-1} = \alpha_n \{(fv)_{j-1/2}^{n-1} - (u^2)_{j-1/2}^{n-1}\} - L_{j-1/2}^{n-1}$

Again from the equation (A13), then

$$\frac{1}{2P_r} h_j^{-1}\left(p_j^n - p_j^n + p_{j-1}^{n-1} - p_{j-1}^{n-1}\right) + \frac{P_1}{2}\left\{(fp)_{j-1/2}^n + (fp)_{j-1/2}^{n-1}\right\}$$
$$- \frac{P_3}{2}\left\{(ug)_{j-1/2}^n + (ug)_{j-1/2}^{n-1}\right\} + \frac{P_5}{4P_r} h_j^{-1}\left[\left(g_{j-1/2}^n + g_{j-1/2}^{n-1}\right)\left(p_j^n - p_{j-1}^n + p_{j-1}^{n-1} - p_{j-1}^{n-1}\right)\right]$$
$$+ \frac{P_5}{2P_r}\left\{(p^2)_{j-1/2}^n + (p^2)_{j-1/2}^{n-1}\right\} + \frac{P_6}{2}\left\{g_{j-1/2}^n + g_{j-1/2}^{n-1}\right\}$$
$$= \frac{1}{2k_n}\xi_{j-1/2}^{n-1}\left[\left(u_{j-1/2}^n + u_{j-1/2}^{n-1}\right)\left(g_{j-1/2}^n - g_{j-1/2}^{n-1}\right) - \left(p_{j-1/2}^n + p_{j-1/2}^{n-1}\right)\left(f_{j-1/2}^n - f_{j-1/2}^{n-1}\right)\right]$$

$$\Rightarrow \frac{1}{P_r} h_j^{-1}(p_j^n - p_{j-1}^n) + (p_1 + \alpha_n)(fp)_{j-1/2}^n - (p_3 + \alpha_n)(ug)_{j-1/2}^n$$
$$+ \frac{p_5}{2P_r} h_j^{-1} g_{j-1/2}^n (p_j^n - p_{j-1}^n + p_j^{n-1} - p_{j-1}^{n-1}) + \frac{p_5}{2P_r} h_j^{-1} g_{j-1/2}^{n-1} (p_j^n - p_{j-1}^n) + \frac{p_5}{P_r}\left(p^2\right)_{j-1/2}^n$$
$$+ P_6 g_{j-1/2}^n + \alpha_n [u_{j-1/2}^n g_{j-1/2}^{n-1} - g_{j-1/2}^n u_{j-1/2}^{n-1} - p_{j-1/2}^n f_{j-1/2}^{n-1} + f_{j-1/2}^n p_{j-1/2}^{n-1}]$$
$$= \alpha_n [(fp)_{j-1/2}^{n-1} - (ug)_{j-1/2}^{n-1}] - M_{j-1/2}^{n-1}$$

where,

$$M_{j-1/2}^{n-1} = \frac{h_j^{-1}}{P_r}\left\{p_j^{n-1} - p_{j-1}^{n-1}\right\} + p_1(fp)_{j-1/2}^{n-1} - p_3(ug)_{j-1/2}^{n-1} + \frac{p_5}{P_r}\left(p^2\right)_{j-1/2}^{n-1} + p_6 g_{j-1/2}^{n-1}$$
$$+ \frac{p_5 h_j^{-1}}{2P_r} g_{j-1/2}^{n-1}\left\{p_j^{n-1} - p_{j-1}^{n-1}\right\}$$

$$\Rightarrow \frac{1}{P_r} h_j^{-1}(p_j^n - p_{j-1}^n) + (p_1 + \alpha_n)(fp)_{j-1/2}^n - (p_3 + \alpha_n)(ug)_{j-1/2}^n$$
$$+ \frac{p_5}{2P_r} h_j^{-1} g_{j-1/2}^n (p_j^n - p_{j-1}^n + p_j^{n-1} - p_{j-1}^{n-1}) + \frac{p_5}{2P_r} h_j^{-1} g_{j-1/2}^{n-1}(p_j^n - p_{j-1}^n) \qquad \text{(A15)}$$
$$+ P_6 g_{j-\frac{1}{2}}^n + \frac{p_5}{P_r}\left(p^2\right)_{j-\frac{1}{2}}^n + \alpha_n[\, u_{j-1/2}^n g_{j-1/2}^{n-1} - g_{j-1/2}^n u_{j-1/2}^{n-1} - p_{j-1/2}^n f_{j-1/2}^{n-1}$$
$$+ f_{j-1/2}^n p_{j-1/2}^{n-1}] = T_{j-1/2}^{n-1}$$

where, $T_{j-1/2}^{n-1} = -M_{j-1/2}^{n-1} + \alpha_n\left\{(fp)_{j-1/2}^{n-1} - (ug)_{j-1/2}^{n-1}\right\}$

The boundary condition becomes

$$f_0^n = 0, \quad u_0^n = 0, \quad p_0^n(\xi,0) = \xi^{\frac{1}{5}}(1+\xi)^{\frac{-1}{5}} g_0^n - 1/(1+\xi)^{\frac{-1}{4}} + \gamma\,\xi^{1/5}(1+\xi)^{\frac{-9}{20}} g_0^n \qquad \text{(A16)}$$
$$u_j^n = 0, \quad g_j^n = 0$$

If assume $f_j^{n-1}, u_j^{n-1}, v_j^{n-1}, g_j^{n-1}, p_j^{n-1}$ to be known for $0 \le j \le J$, equations (A5) to (A15) from a system of 5J+5 non linear equations for the solutions of the 5J+5 unknowns $(f_j^n, u_j^n, v_j^n, g_j^n, p_j^n)$, j = 0, 1, 2, 3,…, J. These non-linear systems of algebraic equations are to be non-linearized by Newton's Quassy linearization method. We define the iterates $(f_j^n, u_j^n, v_j^n, g_j^n, p_j^n)$, n = 0, 1, 2, 3…, N, with initial values equal those at the previous x-station, which are usually the best initial guess available. For the higher iterates, we set

$$f_j^{(i+1)} = f_j^i + \delta f_j^i \qquad \text{(A17)}$$

$$u_j^{(i+1)} = u_j^i + \delta f_j^i \qquad \text{(A18)}$$

$$v_j^{(i+1)} = v_j^i + \delta v_j^i \qquad \text{(A19)}$$

$$g_j^{(i+1)} = g_j^i + \delta g_j^i \qquad \text{(A20)}$$

$$p_j^{(i+1)} = p_j^i + \delta p_j^i \qquad \text{(A21)}$$

Now by substituting the right hand sides of the above equations in place of f_j^n, u_j^n, v_j^n and g_j^n dropping the terms that are quadratic in δf_j^i, δu_j^i, δv_j^i and δp_j^i then the equations (A9), (A10) and (A11) in the following form

$$f_j^{(i)} + \delta f_j^{(i)} - f_{j-1}^{(i)} - \delta f_{j-1}^{(i)} = \frac{h_j}{2}\left\{u_j^{(i)} + \delta u_j^{(i)} + u_{j-1}^{(i)} + \delta u_{j-1}^{(i)}\right\}$$

$$\delta f_j^{(i)} - \delta f_{j-1}^{(i)} - \frac{h_j}{2}(\delta u_j^{(i)} + \delta u_{j-1}^{(i)}) = (r_1)_j \tag{A22}$$

$$\delta u_j^{(i)} - \delta u_{j-1}^{(i)} - \frac{h_j}{2}(\delta v_j^{(i)} + \delta v_{j-1}^{(i)}) = (r_4)_j \tag{A23}$$

$$\delta g_j^{(i)} - \delta g_{j-1}^{(i)} - \frac{h_j}{2}(\delta p_j^{(i)} + \delta p_{j-1}^{(i)}) = (r_5)_j \tag{A24}$$

where, $(r_1)_j = f_{j-1}^{(i)} - f_j^{(i)} + h_j u_{j-1/2}^{(i)}$

$(r_4)_j = u_{j-1}^{(i)} - u_j^{(i)} + h_j v_{j-1/2}^{(i)}$

$(r_5)_j = g_{j-1}^{(i)} - g_j^{(i)} + h_j p_{j-1/2}^{(i)}$

Then equation (A14) becomes,

$$h_j^{-1}\left(v_j^{(i)} + \delta v_j^{(i)} - v_{j-1}^{(i)} - \delta v_{j-1}^{(i)}\right) + \left(\frac{P_1 + \alpha_n}{2}\right)\left\{(fv)_j^{(i)} + \delta(fv)_j^{(i)} + (fv)_{j-1}^{(i)} + \delta(fv)_{j-1}^{(i)}\right\}$$
$$-\left(\frac{P_2 + \alpha_n}{2}\right)\left\{(u^2)_j^{(i)} + \delta(u^2)_j^{(i)} + (u^2)_{j-1}^{(i)} + \delta(u^2)_{j-1}^{(i)}\right\} - \frac{P_4}{2}\left\{(u)_j^{(i)} + \delta(u)_j^{(i)} + (u)_{j-1}^{(i)} + \delta(u)_{j-1}^{(i)}\right\}$$
$$+\frac{1}{2}\left\{g_j^{(i)} + \delta g_j^{(i)} + g_{j-1}^{(i)} + \delta g_{j-1}^{(i)}\right\} + \frac{\alpha_n}{2}\left\{f_j^{(i)} + \delta f_j^{(i)} + f_{j-1}^{(i)} + \delta f_{j-1}^{(i)}\right\} v_{j-1/2}^{n-1}$$
$$-\frac{\alpha_n}{2}\left(v_j^{(i)} + \delta v_j^{(i)} + v_{j-1}^{(i)} + \delta v_{j-1}^{(i)}\right) f_{j-1/2}^{n-1} = R_{j-1/2}^{n-1}$$

$$\Rightarrow \delta v_j^{(i)}\left[h_j^{-1} + \frac{P_1 + \alpha_n}{2} f_j^{(i)} - \frac{\alpha_n}{2} f_{j-1/2}^{n-1}\right] + \delta v_{j-1}^{(i)}\left[-h_j^{-1} + \frac{(P_1 + \alpha_n)}{2} f_j^{(i)} - \frac{\alpha_n}{2} f_{j-1/2}^{n-1}\right]$$
$$+\delta f_j^{(i)}\left[\frac{(P_1 + \alpha_n)}{2} v_j^{(i)} + \frac{\alpha_n}{2} v_{j-1/2}^{n-1}\right] + \delta f_{j-1}^{(i)}\left[\frac{(P_1 + \alpha_n)}{2} v_{j-1}^{(i)} + \frac{\alpha_n}{2} v_{j-1/2}^{n-1}\right]$$
$$+\delta u_j^{(i)}\left[-(P_2 + \alpha_n) u_j^{(i)} - \frac{P_4}{2}\right] + \delta u_{j-1}^{(i)}\left[-(P_2 + \alpha_n) u_{j-1}^{(i)} - \frac{P_4}{2}\right]$$
$$+\delta g_j^{(i)}[1/2] + \delta g_{j-1}^{(i)}[1/2] = (r_2)_j$$

$$\Rightarrow (s_1)_j\,\delta v_j^{(i)} + (s_2)_j\,\delta v_{j-1}^{(i)} + (s_3)_j\,\delta f_j^{(i)} + (s_4)_j\,\delta f_{j-1}^{(i)} + (s_5)_j\,\delta u_j^{(i)} + (s_6)_j\,\delta u_{j-1}^{(i)} + (s_7)_j\,\delta g_j^{(i)} + (s_8)_j\,\delta g_{j-1}^{(i)} + (s_9)_j.0 + (s_1)_j.0 \;= (r_2)_j \tag{A25}$$

where, $(s_1)_j = h_j^{-1} + \dfrac{P_1+\alpha_n}{2} f_j^{(i)} - \dfrac{\alpha_n}{2} f_{j-1/2}^{n-1}$

$$(s_2)_j = -h_j^{-1} + \frac{P_1+\alpha_n}{2} f_j^{(i)} - \frac{\alpha_n}{2} f_{j-1/2}^{n-1}$$

$$(s_3)_j = \frac{(P_1+\alpha_n)}{2} v_j^{(i)} + \frac{\alpha_n}{2} v_{j-1/2}^{n-1}$$

$$(s_4)_j = \frac{(P_1+\alpha_n)}{2} v_{j-1}^{(i)} + \frac{\alpha_n}{2} v_{j-1/2}^{n-1}$$

$$(s_5)_j = -(P_2+\alpha_n) u_j^{(i)} - \frac{P_4}{2}$$

$$(s_6)_j = -(P_2+\alpha_n) u_{j-1}^{(i)} - \frac{P_4}{2}$$

$$(s_7)_j = [1/2]$$

$$(s_8)_j = [1/2]$$

$$(s_9)_j = 0$$

$$(s_{10})_j = 0$$

$$(r_2)_j = R_{j-1/2}^{n-1} - h_j^{-1}\left(v_j^{(i)} - v_{j-1}^{(i)}\right) - \frac{(P_1+\alpha_n)}{2}\left\{(fv)_j^{(i)} + (fv)_{j-1}^{(i)}\right\} + \frac{(P_2+\alpha_n)}{2}\left\{(u^2)_j^{(i)} + (u^2)_{j-1}^{(i)}\right\} + \frac{P_4}{2}(u_j^{(i)} + u_{j-1}^{(i)}) - \frac{1}{2}(g_j^{(i)} + g_{j-1}^{(i)}) - \frac{\alpha_n}{2}(f_j^{(i)} + f_{j-1}^{(i)}) v_{j-1/2}^{n-1} + \frac{\alpha_n}{2}(v_j^{(i)} + v_{j-1}^{(i)}) f_{j-1/2}^{n-1} \tag{A26}$$

Here the coefficients $(s_9)_j$ and $(s_{10})_j$, which is zero in this case, are included here for the generality. Similarly by using the equations (A17) to (A21) then the equation (A15) in the following form

$$\Rightarrow \frac{1}{\Pr} h_j^{-1}\{P_j{}^i + \delta P_j{}^i - P^i{}_{j-1} - \delta P^i{}_{j-1}\} + \frac{(P_1+\alpha_n)}{2}\{(fp)^i_j + \delta(fp)^i_j + (fp)^i_{j-1} + \delta(fp)^i_{j-1}\}$$

$$- \frac{(P_3+\alpha_n)}{2}\{(ug)^i_j + \delta(ug)^i_j + (ug)^i_{j-1} + \delta(ug)^i_{j-1}\} + \frac{P_5 h_j^{-1}}{4\Pr}\{g^i_j + \delta g^i_j + g^i_{j-1} + \delta g^i_{j-1}\}$$

$$\{P^n_j - P^n_{j-1} + P^{n-1}_j - P^{n-1}_{j-1}\} + \frac{P_5 h_j^{-1}}{2\Pr} g^{n-1}_{j-\frac{1}{2}}\{P_j{}^i + \delta P_j{}^i - P_{j-1}{}^i - \delta P_{j-1}{}^i\} + \frac{P_5}{2\Pr}\{(P^2)^i_j +$$

$$\delta(P^2)^i_j + (P^2)^i_{j-1} + \delta(P^2)^i_{j-1}\} + \frac{P_6}{2}\left\{g^i_j + \partial g^i_j + g^i_{j-1} + \partial g^i_{j-1}\right\}$$

$$+ \frac{\alpha_n}{2}[\{u^i_j + \delta u^i_j + u^i_{j-1} + \delta u^i_{j-1}\} g^{n-1}_{j-\frac{1}{2}} - \{g^i_j + \delta g^i_j + g^i_{j-1} + \delta g^i_{j-1}\} u^{n-1}_{j-\frac{1}{2}} - (P^i_j + \delta P^i_j + P^i_{j-1}$$

$$+ \delta P^i_{j-1}) f^{n-1}_{j-\frac{1}{2}} + (f^i_j + \delta f^i_j + f^i_{j-1} + \delta f^i_{j-1}) p^{n-1}_{j-\frac{1}{2}}] \;=\; T^{n-1}_{j-\frac{1}{2}}$$

$$\Rightarrow \delta P^i_j[\frac{h_j^{-1}}{\Pr} + \frac{P_1 P}{2} f^i_j + \frac{P_5 h_j^{-1}}{2\Pr} g^{n-1}_{j-\frac{1}{2}} + \frac{P_5}{\Pr} P^i_j - \frac{\alpha_n}{2} f^{n-1}_{j-\frac{1}{2}}]$$

$$+ \delta P^i_{j-1}[-\frac{h_j^{-1}}{\Pr} + \frac{P_1 P}{2} f^i_j - \frac{P_5 h_j^{-1}}{2\Pr} g^{n-1}_{j-\frac{1}{2}} + \frac{P_5}{\Pr} P^i_j - \frac{\alpha_n}{2} f^{n-1}_{j-\frac{1}{2}}]$$

$$+ \delta f^i_j[\frac{P_1 P}{2} p^i_j + \frac{\alpha_n}{2} P^{n-1}_{j-\frac{1}{2}}] + \delta f^i_{j-1}[\frac{P_1 P}{2} p^i_j + \frac{\alpha_n}{2} P^{n-1}_{j-\frac{1}{2}}]$$

$$+ \delta u^i_j[\frac{P_3 P}{2} g^i_j + \frac{\alpha_n}{2} g^{n-1}_{j-\frac{1}{2}}] + \delta u^i_{j-1}[-\frac{P_3 P}{2} g^i_j + \frac{\alpha_n}{2} g^{n-1}_{j-\frac{1}{2}}]$$

$$+ \delta g^i_j[-\frac{P_3 P}{2} u^i_j + \frac{P_5}{4\Pr}\{P^n_j - P^n_{j-1} + P^{n-1}_j - P^{n-1}_{j-1}\} - \frac{\alpha_n}{2} u^{n-1}_{j-\frac{1}{2}} + \frac{p_6}{2}]$$

$$+ \delta g^i_{j-1}[-\frac{P_3 P}{2} u^i_j + \frac{P_5}{4\Pr}\{P^n_j - P^n_{j-1} + P^{n-1}_j - P^{n-1}_{j-1}\} - \frac{\alpha_n}{2} u^{n-1}_{j-\frac{1}{2}} + \frac{p_6}{2}] \;=\; (r_3)_j$$

$$\begin{aligned}&(t_1)_j\,\delta p^{(i)}_j + (t_2)_j\,\delta p^{(i)}_{j-1} + (t_3)_j\,\delta f^{(i)}_j + (t_4)_j\,\delta f^{(i)}_{j-1} + (t_5)_j\,\delta u^{(i)}_j \\ &+ (t_6)_j\,\delta u^{(i)}_{j-1} + (t_7)_j\,\delta g^{(i)}_j + (t_8)_j\,\delta g^{(i)}_{j-1} + (t_9)_j\,\delta v^{(i)}_j + (t_{10})_j\,\delta v^{(i)}_{j-1} \;= (r_3)_j\end{aligned} \tag{A27}$$

where, $(t_1)_j = \frac{1}{\Pr} h_j^{-1} + \frac{(p_1+\alpha_n)}{2} f^{(i)}_j + \frac{p_5}{2\Pr} h_j^{-1} g^{n-1}_{j-1/2} + \frac{p_5}{\Pr} p^i_j - \frac{\alpha_n}{2} f^{n-1}_{j-1/2}$

$$(t_2)_j = -\frac{1}{\Pr} h_j^{-1} + \frac{(p_1+\alpha_n)}{2} f^{(i)}_{j-1} - \frac{p_5}{2\Pr} h_j^{-1} g^{n-1}_{j-1/2} + \frac{p_5}{\Pr} p^i_{j-1} - \frac{\alpha_n}{2} f^{n-1}_{j-1/2}$$

$$(t_3)_j = \frac{(p_1+\alpha_n)}{2} p^{(i)}_j + \frac{\alpha_n}{2} p^{n-1}_{j-1/2}$$

$$(t_4)_j = \frac{(p_1+\alpha_n)}{2} p^{(i)}_{j-1} + \frac{\alpha_n}{2} p^{n-1}_{j-1/2}$$

$$(t_5)_j = -\frac{(p_3+\alpha_n)}{2} g_j^{(i)} + \frac{\alpha_n}{2} g_{j-1/2}^{n-1}$$

$$(t_6)_j = -\frac{(p_3+\alpha_n)}{2} g_{j-1}^{(i)} + \frac{\alpha_n}{2} g_{j-1/2}^{n-1}$$

$$(t_7)_j = -\frac{(p_3+\alpha_n)}{2} u_j^{(i)} + \frac{p_5}{4\,\mathrm{Pr}} h_j^{-1}\{P_j^n - P_{j-1}^n + P_j^{n-1} - P_{j-1}^{n-1}\} - \frac{\alpha_n}{2} u_{j-1/2}^{n-1} + \frac{p_6}{2}$$

$$(t_8)_j = -\frac{(p_3+\alpha_n)}{2} u_{j-1}^{(i)} + \frac{p_5}{4\,\mathrm{Pr}} h_j^{-1}\{P_j^n - P_{j-1}^n + P_j^{n-1} - P_{j-1}^{n-1}\} - \frac{\alpha_n}{2} u_{j-1/2}^{n-1} + \frac{p_6}{2}$$

$$(t_9)_j = 0$$

$$(t_{10})_j = 0$$

$$\begin{aligned}(r_3)_j \;=\; & T_{j-1/2}^{n-1} - \frac{1}{P_r} h_j^{-1}\left(p_j^{(i)} - p_{j-1}^{(i)}\right) - \frac{(P_1+\alpha_n)}{2}\left\{(fp)_j^{(i)} + (fp)_{j-1}^{(i)}\right\} \\ & + \frac{(P_3+\alpha_n)}{2}\left\{(ug)_j^{(i)} + (ug)_{j-1}^{(i)}\right\} - \frac{P_5}{4\,\mathrm{Pr}} h_j^{-1}(g_j^{(i)} - g_{j-1}^{(i)})\{P_j^n - P_{j-1}^n + P_j^{n-1} - P_{j-1}^{n-1}\} \\ & - \frac{P_5}{2\,\mathrm{Pr}} h_j^{-1}(p_j^{(i)} - p_{j-1}^{(i)}) g_{j-1/2}^{n-1} - \frac{P_5}{2\,\mathrm{Pr}}\left\{(p^2)_j^{(i)} + (p^2)_{j-1}^{(i)}\right\} - \frac{P_6}{2}\left\{g_j^i + g_{j-1}^i\right\} - \\ & \frac{\alpha_n}{2}(u_j^{(i)} + u_{j-1}^{(i)}) g_{j-1/2}^{n-1} + \frac{\alpha_n}{2}(g_j^{(i)} - g_{j-1}^{(i)}) u_{j-1/2}^{n-1} + \frac{\alpha_n}{2}(p_j^{(i)} + p_{j-1}^{(i)}) f_{j-1/2}^{n-1} - \\ & \frac{\alpha_n}{2}(f_j^{(i)} + f_{j-1}^{(i)}) p_{j-1/2}^{n-1}\end{aligned} \tag{A28}$$

The boundary conditions (A16) becomes

$$\begin{aligned}& \delta f_0^n = 0, \qquad \delta u_0^n = 0, \\ & \delta p_0^n(\xi,0) = \delta\left[\xi^{\frac{1}{5}}(1+\xi)^{\frac{-1}{5}} g_0^n - 1/(1+\xi)^{\frac{-1}{4}} + \gamma\xi^{1/5}(1+\xi)^{\frac{-9}{20}} g_0^n\right], \\ & \delta u_j^n = 0, \qquad \delta g_j^n = 0\end{aligned} \tag{A29}$$

Which just express the requirement for the boundary conditions to remain during the iteration process.

Now the system of linear equations (A22), (A23), (A24), (A25) and (A27) together with the boundary conditions (A29) can be written in a black matrix form a coefficient matrix, which are solved by modified " Keller Box " methods especially introduced by Keller (1978). Later, this method has been used most efficiently by Cebeci and Bradshow (1984) and recently by Hossain (1992). Hossain et. al. (1994), taking the initial iteration

to be given by convergent solution at $\xi = \xi_{j-1}$. Results are shown in graphical form by using the numerical values obtained from the above technique. The whole procedure, namely reduction to first order followed by central difference approximations, Newton's Quasi linearization method and the block Thomas algorithm, is well known as Keller-box method.